NASA Contractor Report 166443

USAAVRADCOM TR 83-A-4

(NASA-CR-166443) INTEGRATED TECHNOLOGY ROTOR/FLIGHT RESEARCH ROTOR (ITR/FRR) CONCEPT DEFINITION (Textron Bell Helicopter) 85 p HC A05/MF A01 CSCL 01C

N85-18978

Unclas

G3/05 14911

INTEGRATED TECHNOLOGY ROTOR/FLIGHT RESEARCH ROTOR (ITR/FRR) CONCEPT DEFINITION

James H. Harse

Contract DAAK51-81-C-0026
March 1983

Date for general release March 1985

NASA

US ARMY AVRADCOM

NASA Contractor Report 166443

USAAVRADCOM TR 83-A-4

INTEGRATED TECHNOLOGY ROTOR/FLIGHT RESEARCH ROTOR (ITR/FRR) CONCEPT DEFINITION

James H. Harse
Bell Helicopter Textron Incorporated
Fort Worth, TX 76101

Prepared for
U.S. Army Research and Technology
Laboratories (AVRADCOM)
under Contract DAAK51-81-C-0026

[redacted] Date for general release, March 1985

National Aeronautics and
Space Administration

Ames Research Center
Moffett Field, California 94035

United States Army
Aviation Research and
Development Command
Research and Technology
Laboratory
Moffett Field, California 94035

PREFACE

A program for the Concept Definition study of the ITR/FRR was conducted for the Aeromechanics Laboratory (AL), Moffett Field, California, and Applied Technology Laboratory (ATL), Fort Eustis, Virginia of U.S. Army Research and Technology Laboratories (AVRADCOM) and for the NASA Ames Research Center (ARC), Moffett Field, California. The key Government personnel were Robert A. Ormiston and William G. Bousman of AL, Robert W. Powell and Paul H. Mirick of ATL, and James C. Biggers of NASA ARC.

The key Bell Helicopter Textron Incorporated personnel were James H. Harse (Project Engineer), Peter A. Reyes, James L. Braswell, and William D. Neatherly.

PRECEDING PAGE BLANK NOT FILMED

TABLE OF CONTENTS

TABLE OF CONTENTS (Concluded)

LIST OF FIGURES

LIST OF FIGURES (Concluded)

LIST OF TABLES

1. SUMMARY

This report is for the Concept Definition study for the ITR/FRR program. A program of rotor hub concept development has been performed by Bell Helicopter Textron Incorporated (BHTI) to identify and evaluate a variety of candidate rotor hub configurations. This program was conducted for ATL, AL, and NASA ARC under Contract DAAK51-81-C-0026. The Government's Rotor Hub Design Specifications and Technical Goals (see appendix) were reviewed and hub design loads and blade parameters were established as criteria for the hub concepts. Eight hub concepts were examined and two were selected for refinement. The selected hub concepts were evaluated relative to the technical goals, and their manufacturing aspects were assessed. In addition, hub features that could be varied for the FRR were identified and Rotor Systems Research Aircraft (RSRA) considerations were addressed.

2. INTRODUCTION

Bearingless rotor hubs have the potential for significant improvements in weight, drag, simplicity, reliability, and cost over conventional rotor hubs that are in production today. However, bearingless rotor technology is not adequate to allow production with acceptable risk. Since there is a high probability that bearingless rotors will be incorporated in the ITR/FRR systems, acceptable candidate hub concepts need to be identified. These hub concepts must provide proper flapping and torsional stiffnesses, stability, and strength while achieving the ITR/FRR objectives.

The concept definition phase of the ITR/FRR program provided the opportunity to consider a number of bearingless rotor hub concepts and assess their advantages and disadvantages. BHTI's experience in hingeless and bearingless rotor designs served as the foundation for the generation of hub concepts. The ITR/FRR Rotor Hub Design Specifications and Technical Goals guided the development of the hub concepts and served as the basis for their evaluation. Each hub concept and the methodology used in refining it are described in this report. The concept development is shown in Figure 1. Eight potential hub concepts were qualitatively evaluated and two were selected for further refinement. The two selected hub concepts underwent a merit function evaluation where their physical properties relative to the technical goals were assessed. FRR variations and RSRA compatibility for each selected hub concept were also addressed.

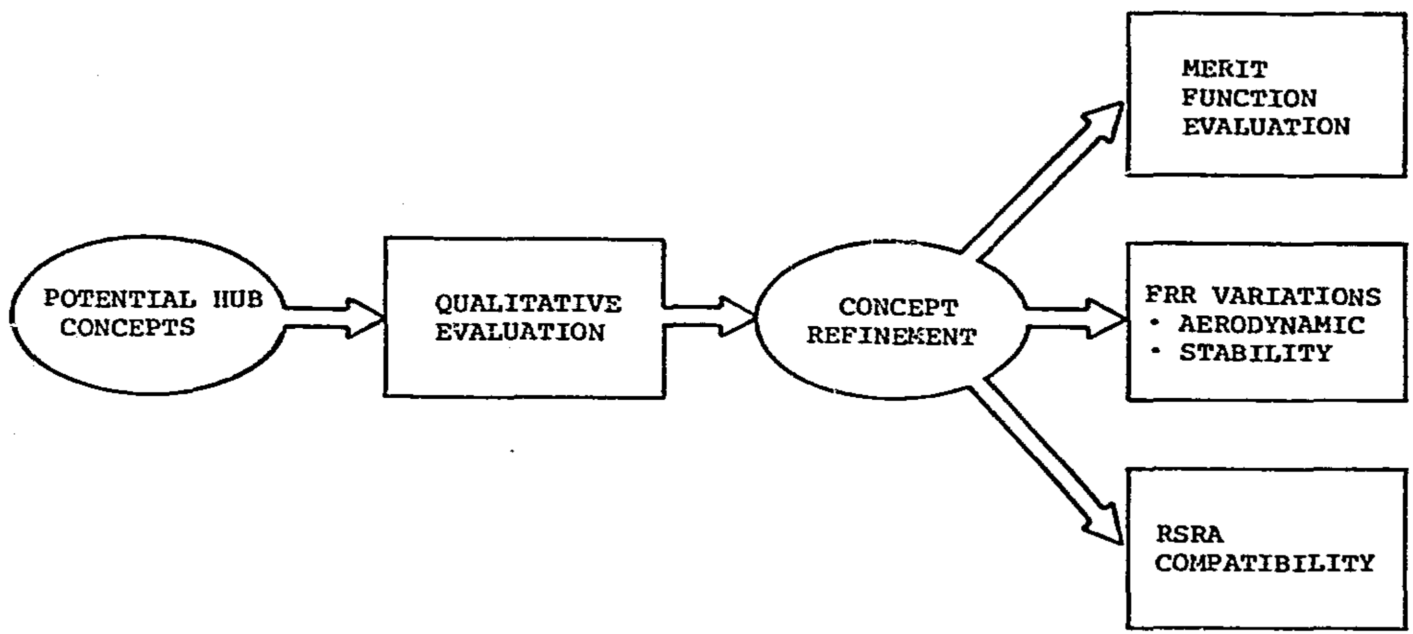

Figure 1. Concept Flowchart

3. HUB DESIGN CRITERIA

3.1 GOALS AND SPECIFICATIONS

The ITR/FRR rotor hub design specifications and technical goals contained in Appendix B of RFQ DAAK51-81-Q-0054 were reviewed as required by Task I of the Statement of Work.

3.1.1 Rotor Hub Design Specifications

BHTI concurs with the specifications with the exception of the requirement regarding survivability of the hub when subjected to the strike of a 23-mm HEI projectile. There are, however, certain impacts of the specifications which warrant further consideration.

3.1.1.1 Rotor Hub Configuration - Blade Folding. Any requirement to provide blade folding will cause an increase in hub weight and drag. The lug which supports the folding blade must carry the load of the blade throughout the folding motion, requiring a considerably stronger (and heavier) lug than would otherwise be necessary. It is also very difficult to create a desirable hub configuration that simultaneously provides for blade folding and cuffs integral with the blade. If cuffs are not integral with the blade, all of the blade chordwise loads must be carried by the blade attachment lugs, and lug size (and chordwise spacing) must be increased accordingly, resulting in more increased weight and drag. The penalty which one must pay for blade folding is also affected by the type of folding required. The requirement to fold two blades 90 degrees (one forward, opposite blade aft) and align the other opposing pair with the fuselage, such as might be required for storage, is much less demanding than to require that all blades be folded aft, such as might be required for shipment. BHTI elected to use the more stringent requirement of folding all blades aft in order to maintain a transportable configuration without blade removal.

3.1.1.2 Rotor Hub Configuration - Surviving a 23-mm HEI Strike. The specification regarding surviving a strike by a 23-mm HEI projectile may be difficult to satisfy because, unlike blades, large portions of the exposed areas of a main rotor hub are highly stressed. This is particularly true of the hub yoke. The yoke of a rotor hub is the primary structural element that carries the centrifugal force of the rotor blades and attaches to the mast. For bearingless rotor hubs, the inboard portion of the yoke forms a flexure that accommodates the flapping motions and the outboard portion of the yoke forms a torsionally soft element that accommodates pitch change motions. Some composite materials are well-suited for main rotor hub construction because they exhibit a very large resistance to crack growth and can allow a fail-safe yoke design that can operate for many hours after some forms of failure. However, if a strike by a 23-mm HEI round is taken by the yoke, catastrophic failure will likely occur quickly, regardless of the cleverness of the design. Any attempt to design a yoke to tolerate such damage will probably result in a weight increase out of proportion to the protection that can be provided, and could preclude obtaining satisfactory stiffnesses and stress levels. One argument favoring the use of a cuff is that it could trigger detonation of the round, providing a measure of protection for the yoke. However, if the strike is by a delayed-fuse round, the cuff may actually contribute to yoke damage by confining the blast. Since a composite hub is likely to emerge as the leading ITR candidate, we feel that it would be realistic to accept the idea that in spite of its many advantages, a composite hub probably cannot be made as survivable to projectile strikes as a metal hub. The 23-mm HEI survivability requirement should be considered a secondary requirement.

3.1.2 Rotor Hub Technical Goals

BHTI concurs with the technical goals; however, for the purpose of clarification, some of the goals are discussed in the following paragraphs.

3.1.2.1 Rotor Hub System Parts Count. This goal is quite conservative. A composite bearingless hub need only have 30 to 40 nonstandard parts, including cone sets, mast plates, and blade attachment bolts. For example, the BHTI Model 680 (a composite bearingless main rotor hub presently undergoing testing) is comprised of only 38 nonstandard parts. These are the parts or sets of subassemblies that are listed in the rotor installation drawing. This will be discussed later in this report.

3.1.2.2 Minimum Rotor Hub Tilt Angle. To evaluate this goal, BHTI Model 412 data were extrapolated to 170 knots. The resulting flapping with respect to the mast ranged from 4 to 8 degrees, depending on gross weight, center-of-gravity location, attitude, and elevator incidence. Assuming that the ITR vehicle will have a favorable combination of mast and transmission flexibilities, and other dynamic and aerodynamic values, 5 degrees of rotor flapping without fatigue damage appears to be a reasonable goal.

3.1.2.3 Auxiliary Lead-Lag Damping. The goal of no auxiliary damping is desirable if it can be attained without unacceptable compromises in rotor characteristics. The ability of fixed kinematic couplings to provide adequate damping under all flight conditions may be difficult to demonstrate. Extensive analysis and model testing must attend any attempt to develop a damperless bearingless yoke and, if such a concept is selected, some form of "fallback" damping should be provided. BHTI's experience has shown that elastomeric dampers can be incorporated into conventional and bearingless hubs with an insignificant impact on the cost and weight. These dampers have high reliability and do not compromise the other functions of the hub while providing the necessary stability. The most appropriate rotor hub for the ITR will fall out of detailed evaluations when the hubs are treated as entire systems.

3.1.2.4 Torsional Stiffness. The goal of no substantial increase in blade pitch control actuation force over that existing in current rotor systems is highly desirable. However, the major contribution to steady control force in the control system is the centrifugal restoring ("tennis racquet") moment generated by the blades, with the torsional stiffness of the yoke playing a smaller part. To speak of control system force, one must speak of the entire rotor. Magnitudes of centrifugal restoring moments and total feathering moments of some current rotor systems are presented later in this report.

3.1.2.5 Rotor Hub System Fatigue Life/Reliability. Both the hub system fatigue life goal and the reliability goal appear to be reasonable, with the possible exception of the elastomeric components. Data are not available to adequately define the endurance life of such materials or to predict the loads that will be imposed on them. However, since they constitute only a small portion of the hub hardware and are easily replaceable, they are of minor importance insofar as these two goals are concerned.

3.2 ROTOR SIZING

BHTI is considering a demonstration of the ITR on the Model 214ST helicopter. This requires the diameter to be not more than 52 feet. The tipspeed and chord must be large enough for the ITR to meet the maneuverability specification of 1.75g from 170 KTAS. But it is desirable to have the tipspeed and chord as low as possible for noise, advancing blade Mach number, centrifugal force, blade weight, and hover performance considerations. For this concept definition effort, the rotational speed, radius, and blade weight are very important because they affect the amount of unidirectional material required, tension in the hub, and both static droop and dynamic loads.

An increase of material in a hub will cause a wider and/or thicker flap flexure. This will result in a higher hub stiffness and increased size of the pitch change cuffs. Also, increased area in the pitch change elements results in higher torsional rigidity and shear stresses due to increased thicknesses. An increase of tension in the hub will provide higher hub moments for a given flap angle. This will increase the size and weight of the hub attachment hardware and blade attachment lugs.

Since the latest methodologies and advanced airfoils will be utilized in the subsequent phases of the ITR program, the chord and tipspeed were established so that the ITR would fall just under the stall losses curve on the rotor thrust coefficient versus advance ratio plot shown in Figure 2. BHTI Model 214ST and UH-60A parameters are also shown in the figure. The resulting ITR tipspeed and thrust-weighted chord are 675 feet per second and 26 inches, respectively. With these parameters, the ITR should be able to perform in the specified maneuver.

3.3 BLADE PARAMETERS

Since the ITR blades will have tapered thickness and chord distributions, some blade parameters necessary for hub development were based on scaling the BHTI Model 680 blades. It is assumed that the ITR blades will have the same thicknesses (skin, core, spar, bondlines, abrasion protection, etc.); therefore, the weight per inch was scaled by the ratio of the thrust-weighted chords. The remaining blade parameters were based on the radius and rotor speed ratios and are presented in Table I. The Model 680 and Model 214ST parameters are also shown for reference.

TABLE I. ROTOR PARAMETERS

	ITR	M680	M214ST
Design Gross Weight (lb)	16,000	7,650	17,500
Blades	4	4	2
Chord (in)	26	13.7	33
Radius (ft)	26	19.875	26
Tipspeed (ft/sec)	675	724	781
Rotor Speed (rpm)	248	348	287
Blade Weight (lb)	210*	85	521
Droop Moment (ft-lb)	3,796	1,169	6,466
Inertia (slug-ft^2/blade)	1,903	448	3,133
Centrifugal Force (lb)	80,000	47,755	181,685

*The ITR goal is 180 lb, but it was considered too optimistic for this effort so the more conservative value was used.

3.4 DESIGN LOADS

The remaining information required for hub development is the beam, chord, and torsion loads or excursions that will be encountered at maximum cruise speed (170 KTAS). It is this high cycle loading, together with the centrifugal force, that governs the

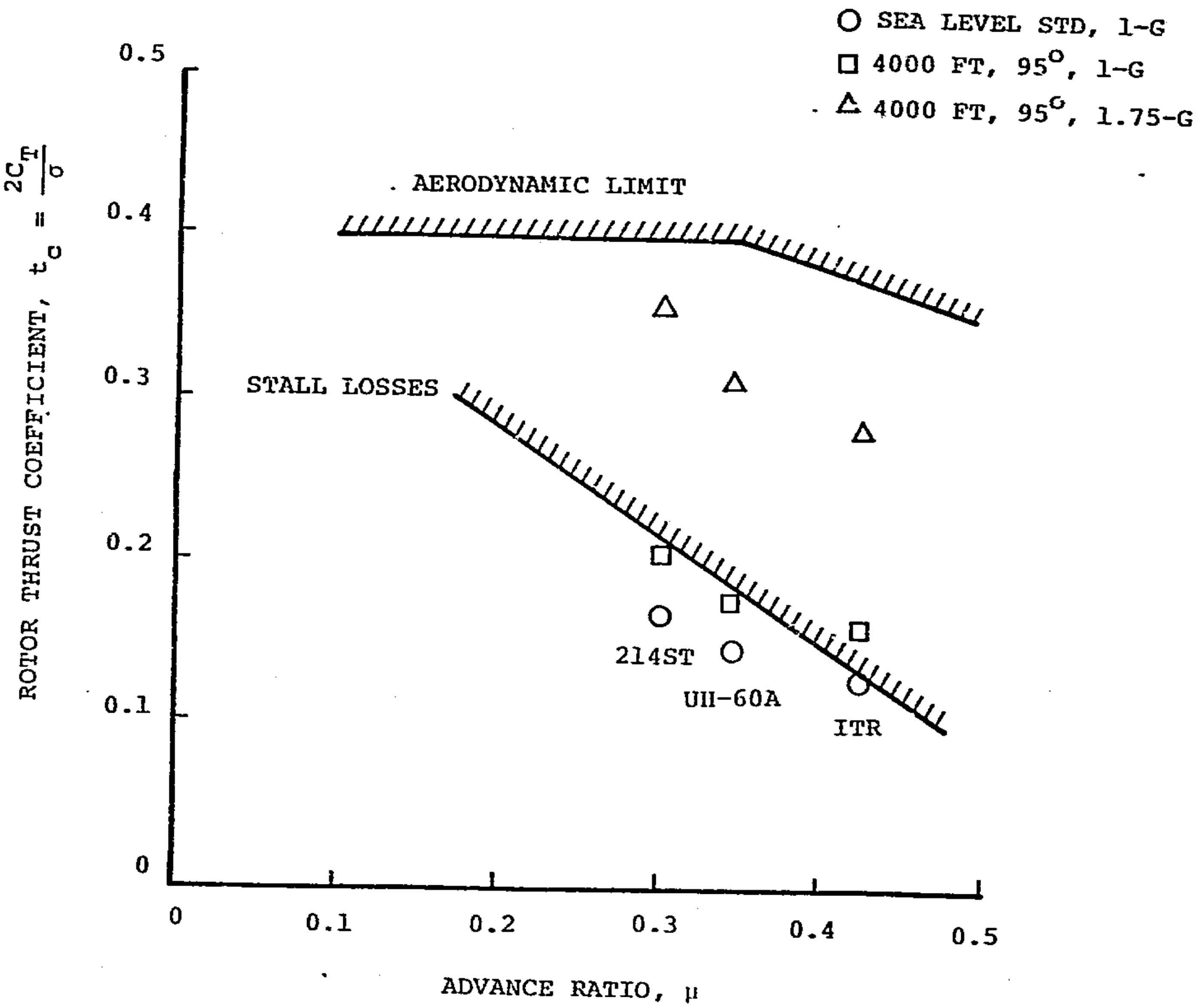

Figure 2. Rotor Thrust Coefficient vs Advance Ratio

design of the key hub components. Maneuvering flight conditions will produce maximum excursions but so few fatigue cycles that this condition does not drive the design.

Table II shows the design loads and motion ranges which were used in the hub concept development.

TABLE II. DESIGN LOADS AND RANGES

Pitch Range	±24 deg
Flapping	±5 deg
Lead-Lag	±0.6 deg
Blade Attachment Lug Loads	
Beam	11,650 ± 12,350 in-lb
Chord	-3,500 ± 30,523 in-lb

The pitch range of 18 degrees collective and ±15 degrees cyclic is the same as that of the BHTI Model 680. This should be adequate to perform the ITR maneuvers and provide a margin of safety for the pitch change element. The flap excursion of ±5 degrees was established by the ITR technical goals.

The lead-lag motion and blade attachment lug loads were based on scaling measured Model 412 loads. BHTI's experience has shown that flight loads will scale by the ratio of the product of velocities squared, radius and gross weight. The Model 412 has a gross weight of 11,500 pounds and a radius of 23 feet; its maximum loads were measured at 132 KTAS. Therefore, the ITR loads are expected to be 2.6 times those of the Model 412.

4. PRELIMINARY HUB CONCEPTS

4.1 CONCEPT DESCRIPTION

Eight potential hub concepts were generated for consideration (see Table III). From these concepts, two were selected for further refinement. The following paragraphs describe the concepts.

4.1.1 Bearingless/Damperless (Concept #1)

The first concept is shown in Figure 3. It is a damperless design without pitch change bearings. It has a one-piece yoke with an inboard flap flexure with a moderate amount of hub moment stiffness to withstand the blade droop loads and augment aeroelastic couplings. The pitch change element is twisted to provide flap/lag coupling and has an offset shear center to induce pitch/lag coupling. This design uses a shear restraint and a torque tube instead of a cuff to introduce blade pitch. A cuff would have a lower drag coefficient but would interfere with the required couplings. A shear restraint is incorporated to effect reduced control loads, pitch washout, and bending stresses at the torque tube/blade interface.

4.1.2 Bearingless/Outboard Blade Attachment (Concept #2)

The second hub concept has a one-piece yoke with an inboard flap flexure with low hub moment stiffness and an outboard pitch change element. A rigid cuff, which attaches at the yoke/blade joint, is used to introduce blade pitch. A shear restraint is incorporated in this design and attached to the yoke. Elastomeric dampers are positioned between the shear restraint and the cuff for stability. This hub concept is shown in the upper portion of Figure 4. The lower portion of the figure shows the hub concept as if there were no requirement for folding, which allows fairing of the blade attachment bolts and produces lower drag and weight.

4.1.3 Bearingless/Inboard Blade Attachment (Concept #3)

The third hub concept has a flap flexure that terminates into lugs where the pitch change element attaches. The pitch change element is integral with the blade spar and the cuff is integral with the blade skins for reduced drag. A shear restraint and dampers are used in this design, shown in Figure 5. One disadvantage of this design is that the attachment lugs tend to get larger as they are moved inboard, thus affecting the functional ability of the flap flexure. Also, with the inboard attachment joint, the blades are limited to approximately 90 degrees folding and the pitch link must be disconnected when the blades are folded.

TABLE III. PRELIMINARY HUB CONCEPTS

Hub Concept Number							
1	2	3	4	5	6	7	8
Bearingless						Pitch Change Bearings	
Flap Flexure				Flap Hinge			
Damperless	Outboard Attachment	Inboard Attachment	Short Pitch Change Element	Gimbal	Offset	Tension Loaded Flap Flexure	Unloaded Flap Flexure

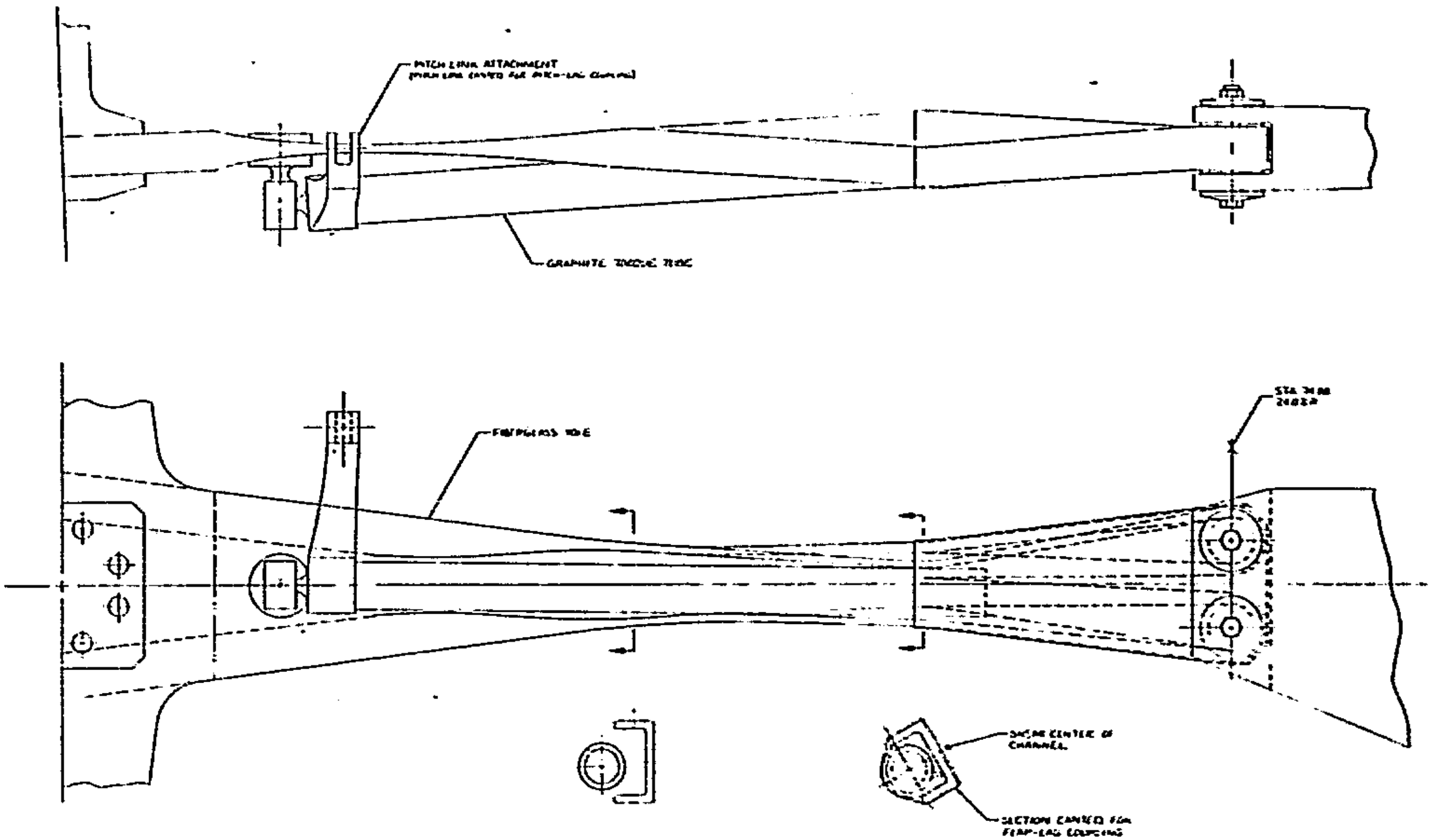

Figure 3. Bearingless/Damperless Hub Concept No. 1

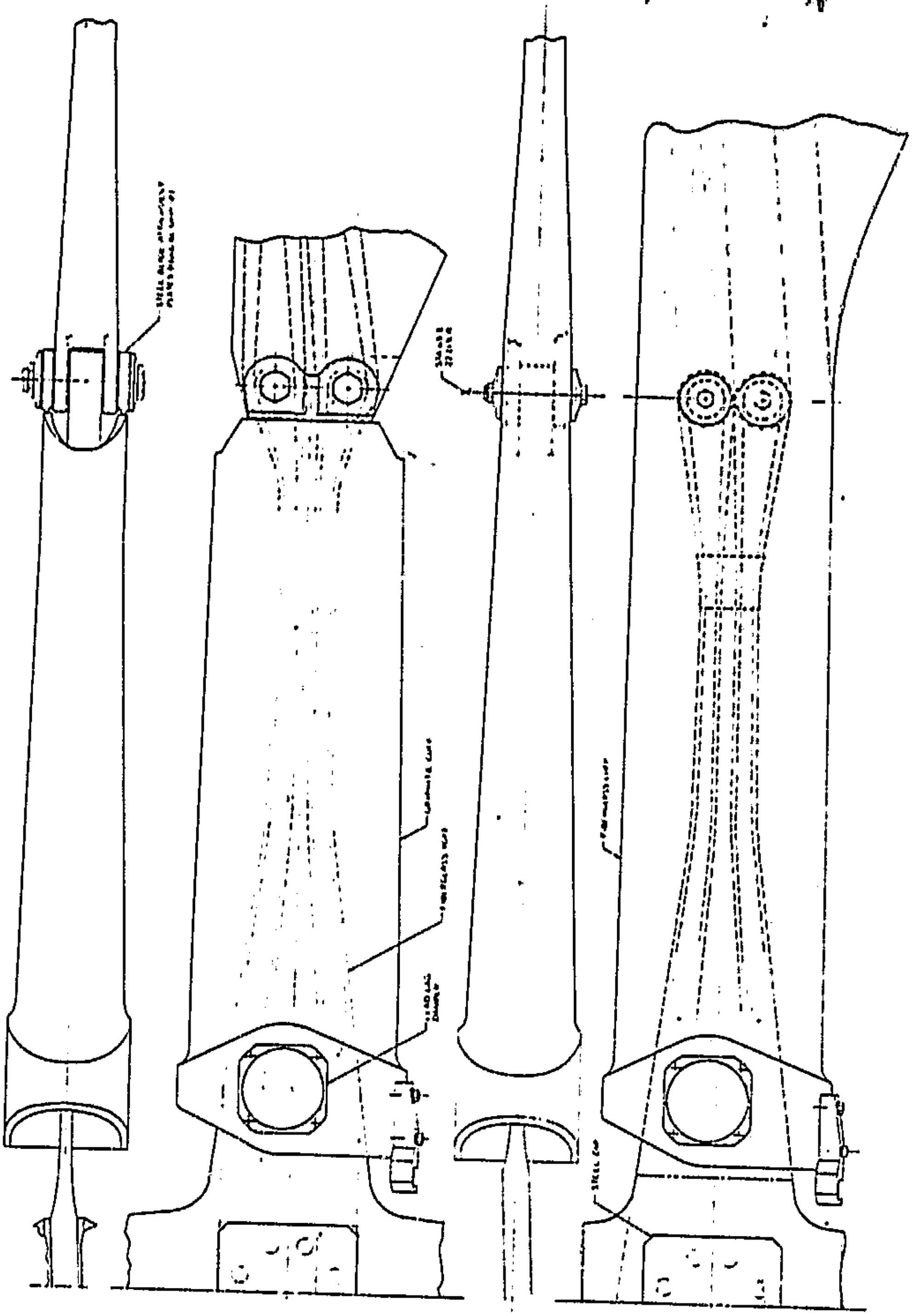

Figure 4. Bearingless/Outboard Blade Attachment Hub Concept No. 2

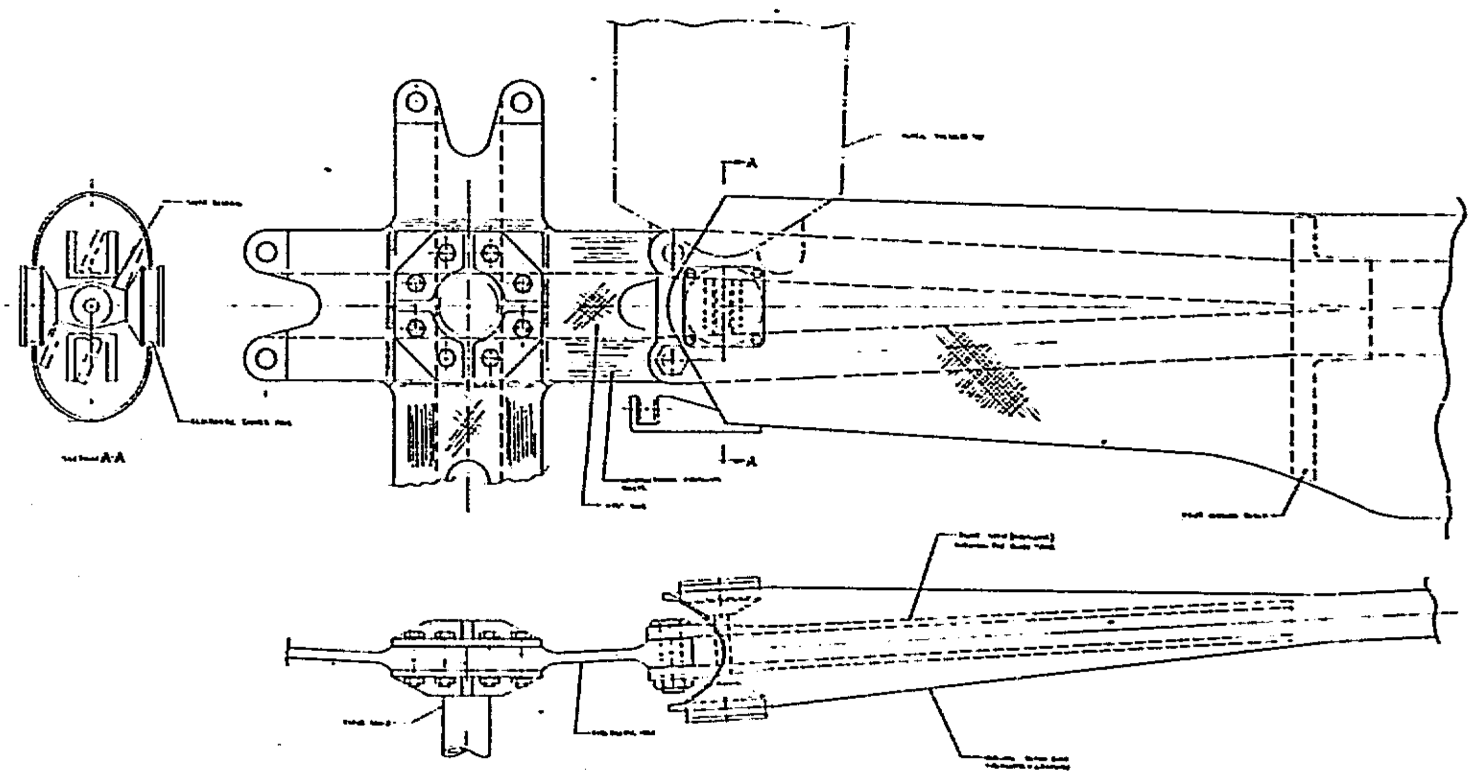

Figure 5. Bearingless/Inboard Blade Attachment Hub Concept No. 3

4.1.4 Bearingless/Short Pitch Change Element (Concept #4)

The fourth design is an attempt to reduce the length of the pitch change element with elastomer laminated between glass belts for reduced torsional stiffness (Figure 6). With the shorter yoke, a cuff/damper arrangement would not provide the displacements necessary for damping, as in the other concepts. Therefore, a torque tube is used and the dampers are attached to the hub clamp plates and exercised by axial motion of the torque tube as the blades lead and lag. Other considerations would be droop and "S" bending in the yoke.

4.1.5 Bearingless/Gimbal (Concept #5)

The fifth hub concept (Figure 7) is a gimbaled design with elastomeric hub spring to meet the flapping goals without a droop stop. A coning flexure will carry the droop loads and attach to the pitch change element, shear restraint, damper and cuff arrangement in the same manner as in hub concept #3. This gimbaled design would have the same folding limitations as #3 and would also have a large amount of pitch/flap coupling.

4.1.6 Bearingless/Offset Flap Hinge (Concept #6)

The sixth hub concept, shown in Figure 8, is a design with an offset flapping hinge to better meet the hub moment stiffness goals and larger flapping angles. Fiberglass belts are attached to the flapping bearings and form a pitch change element. The belts terminate into lugs where the blade and a cuff are attached. This design also incorporates a shear restraint and dampers.

4.1.7 Pitch Change Bearings/Tension Loaded Flexure (Concept #7)

The seventh hub concept, shown in Figure 9, is a design with a flap flexure, elastomeric pitch change bearings, and an elastomeric damper for reduced risk. This design can provide the maximum amount of damping and offers the lowest stresses due to flapping for a tension-loaded flexure.

The yoke is a one-piece fiberglass structure and offers fail-safe features, as do the yokes in the previous hub concepts. However, the pitch change bearings must be large enough to react the centrifugal force and chord loads.

4.1.8 Pitch Change Bearings/Unloaded Flexure (Concept #8)

The eighth hub concept, shown in Figure 10, is a design with the centrifugal force transmitted from the pitch change bearings to the hub clamp plates, thus unloading the flap flexure. This offers the minimum risk for the flapping loads and will be better

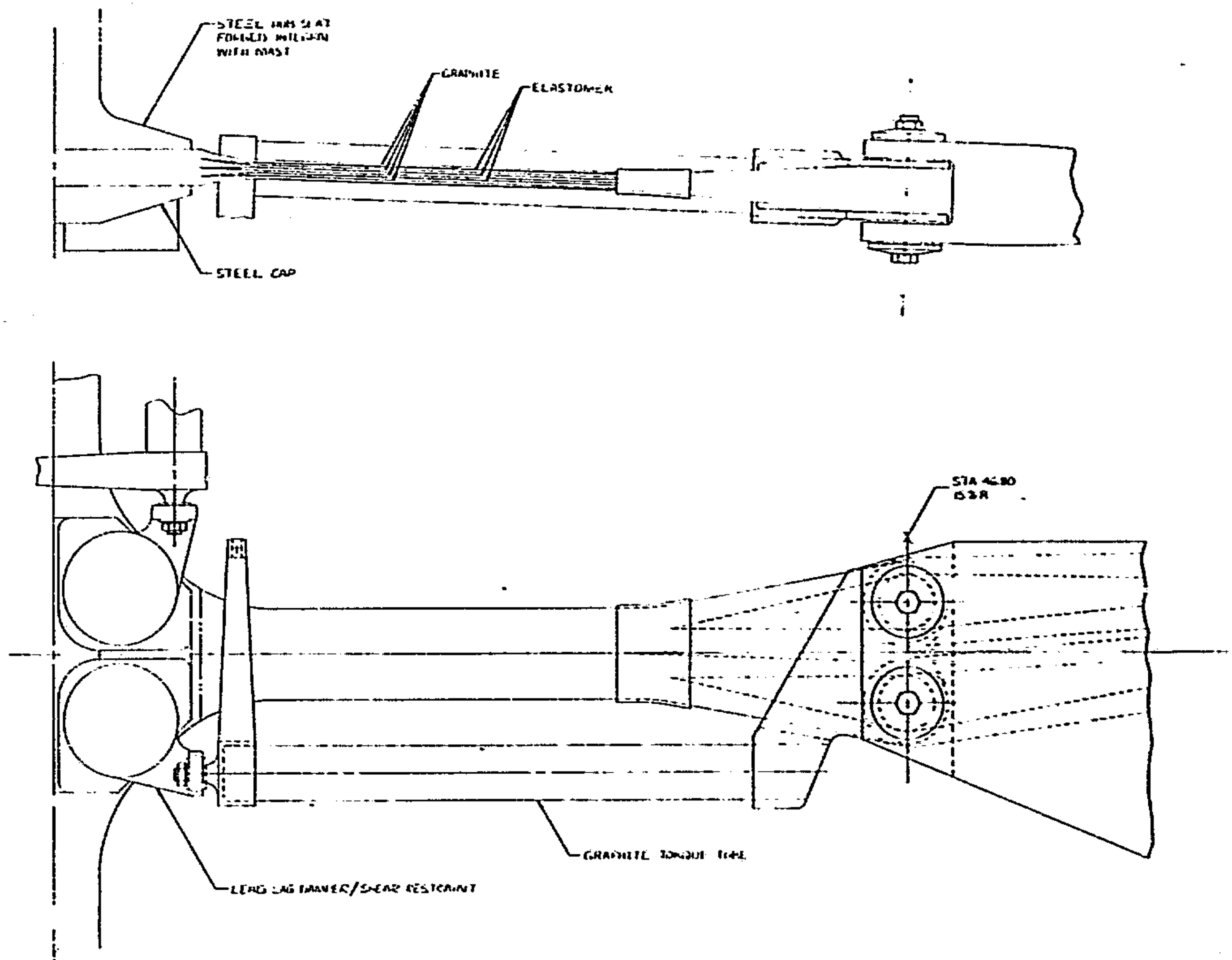

Figure 6. Bearingless/Short Pitch Change Element Hub Concept No. 4

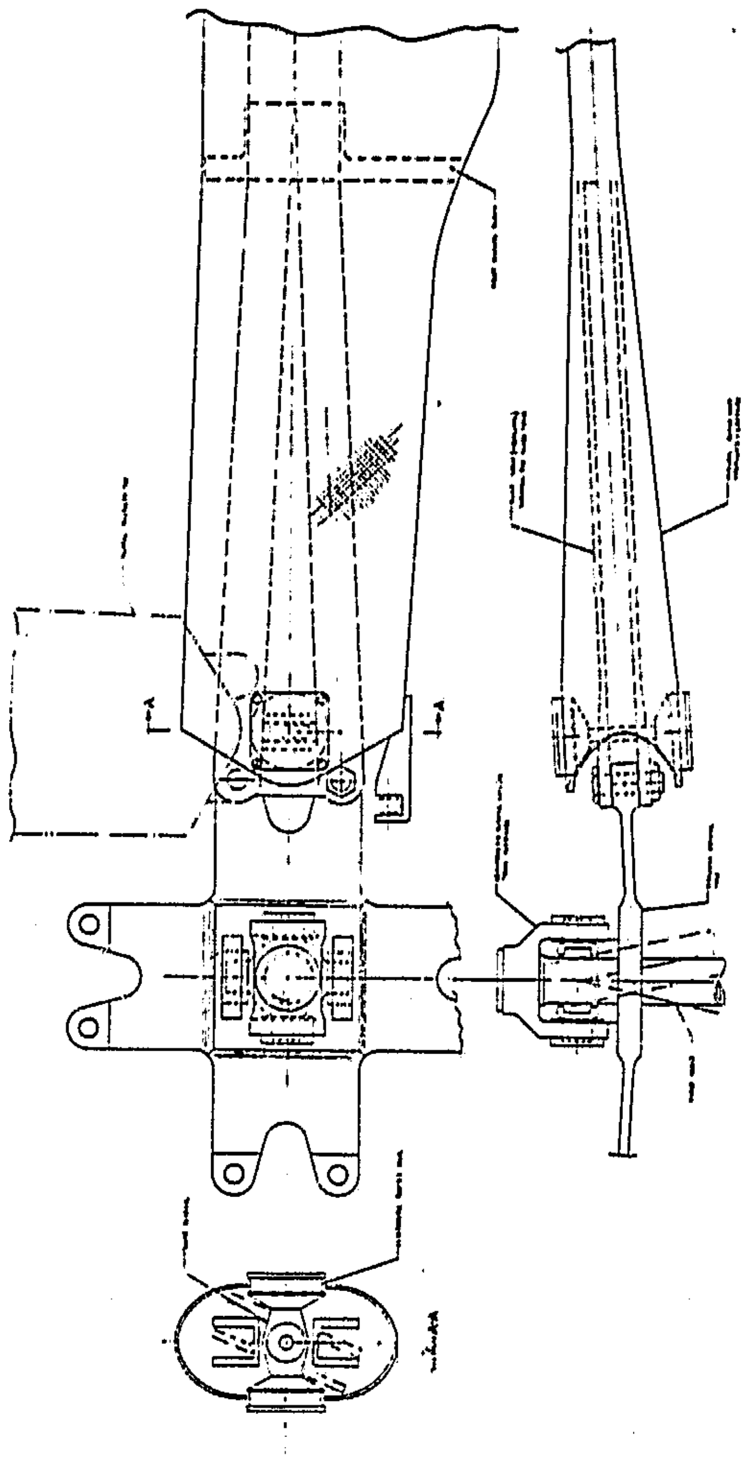

Figure 7. Bearingless/Gimbal Hub Concept No. 5

ORIGINAL PAGE IS
OF POOR QUALITY

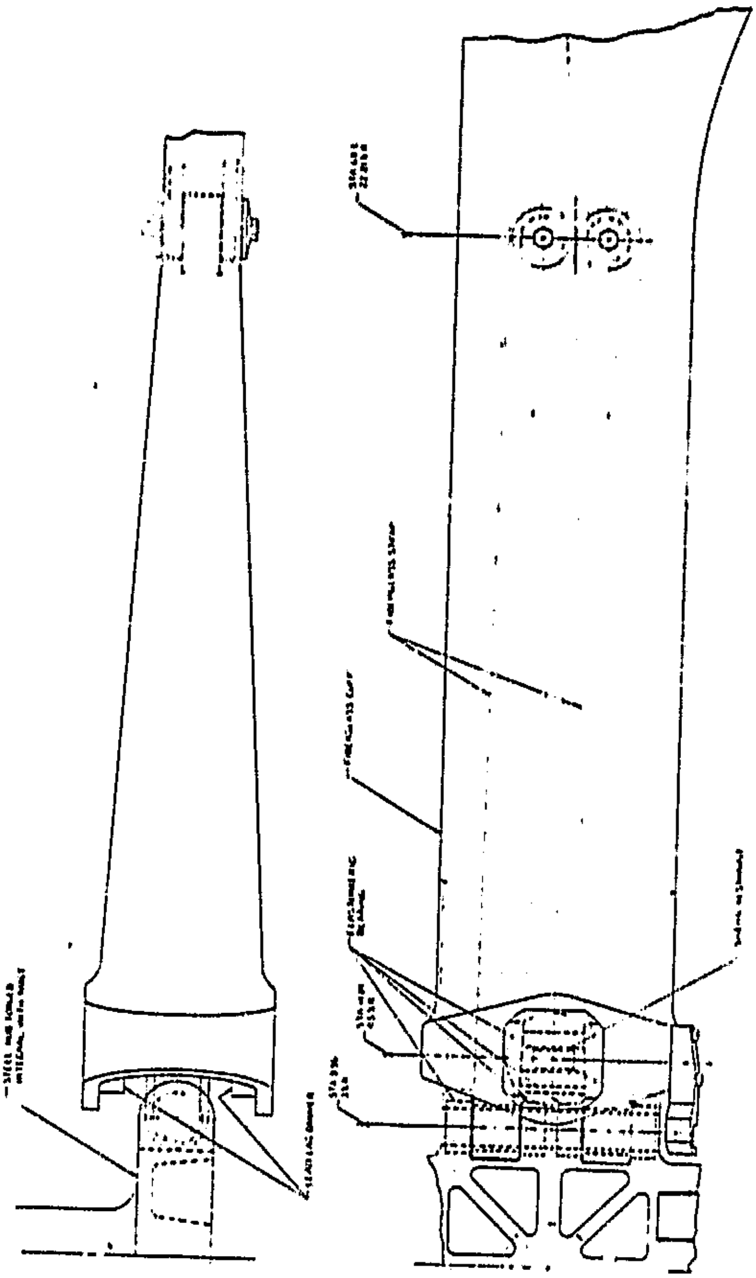

Figure 8. Bearingless/Offset Flap Hinge Hub Concept No. 6

ORIGINAL PAGE IS
OF POOR QUALITY

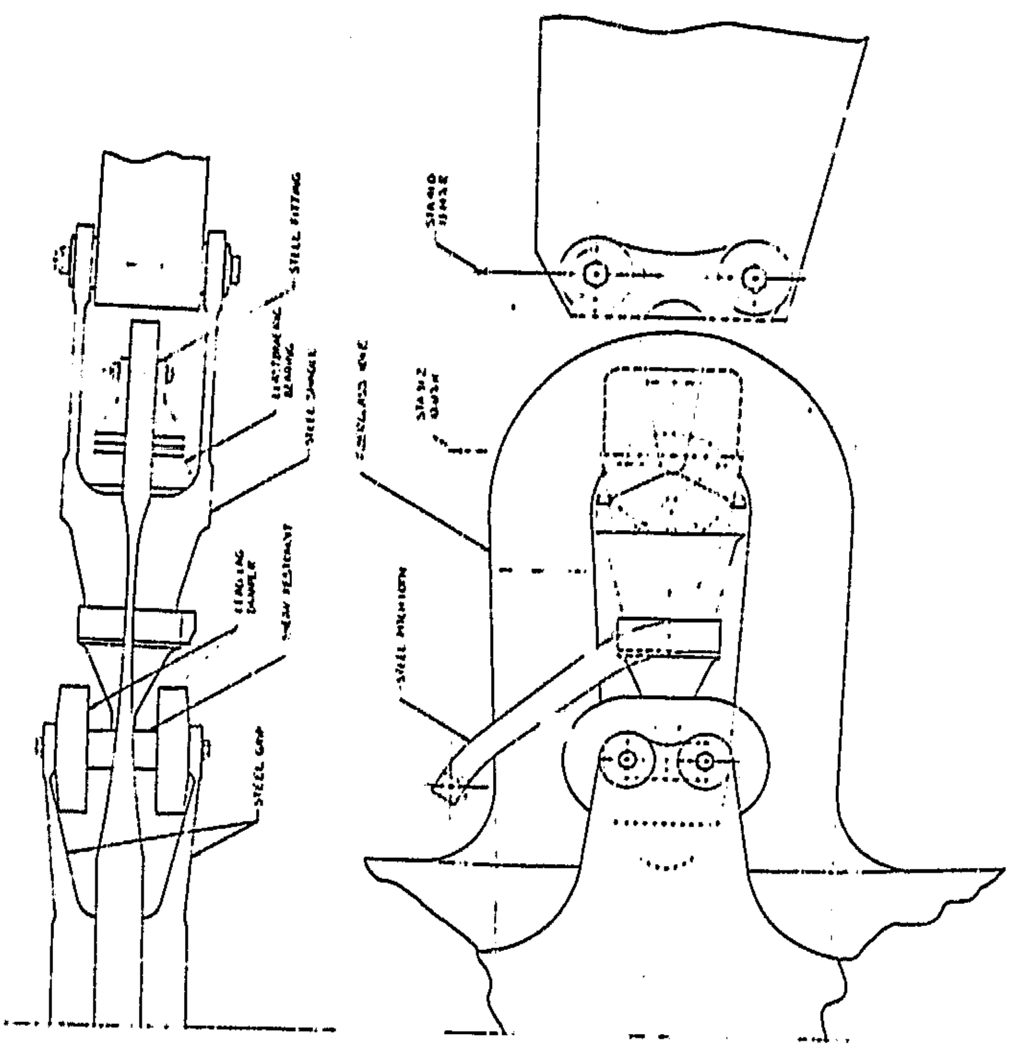

Figure 9. Pitch Change Bearings/Tension Loaded Flexure Hub Concept No. 7

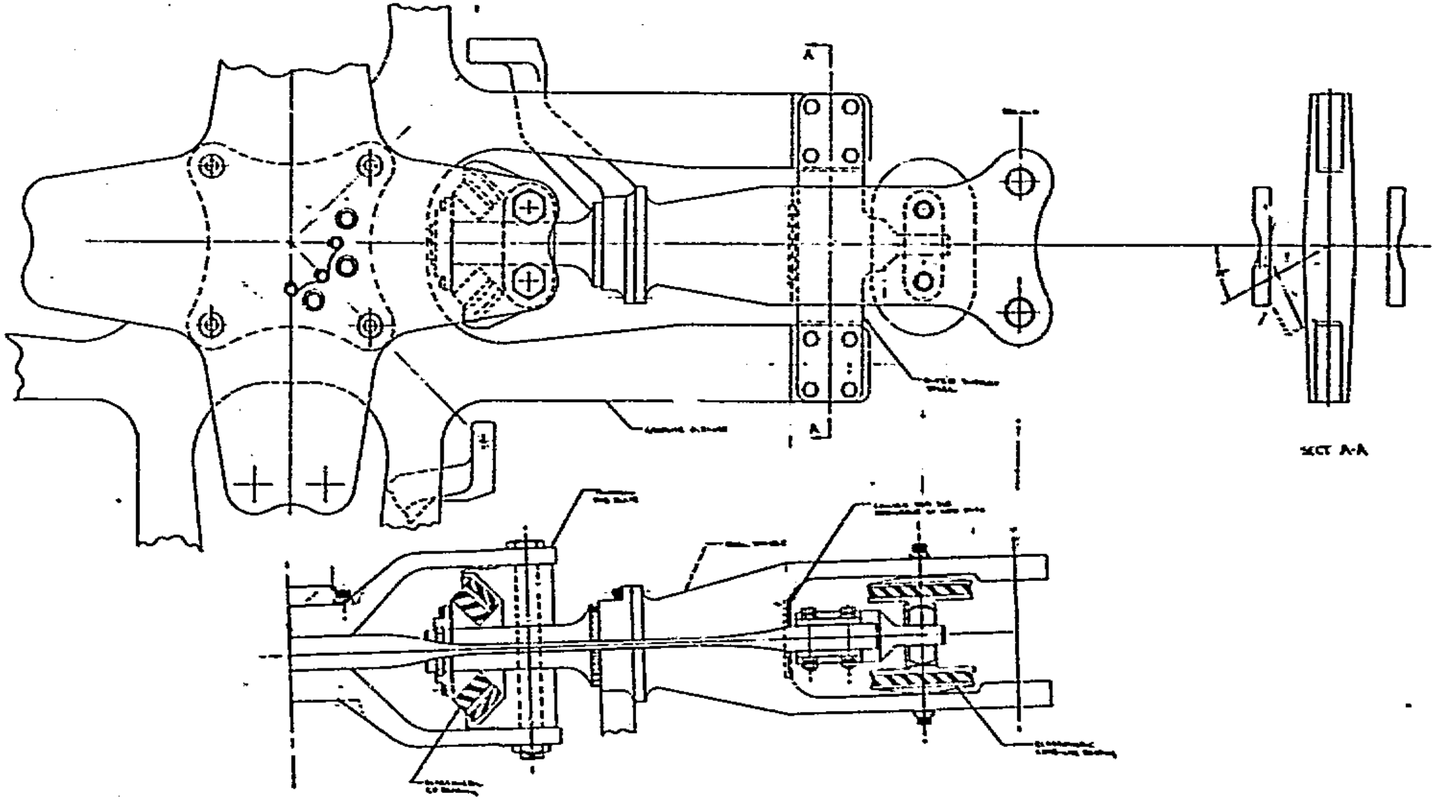

Figure 10. Pitch Change Bearings/Unloaded Flexure Hub Concept No. 8

able to meet the hub moment stiffness goal. The flap flexure is graphite for reduced yoke weight; however, the clamp plates and pitch bearings will be large.

4.2 HUB CONCEPT SELECTION

To select two hub concepts for refinement in the subsequent tasks, copies of the eight hub concepts were given to 23 BHTI engineers in the Rotor Design, Rotor Stress, Flight Technology, and Research groups. They were asked to rate each hub concept from 1 to 10 on survivability, risk, cost, drag, and weight. The engineers were asked to base their ratings on the potential of each hub concept once it is refined. The results are shown in Table IV. Also shown in the table are weighted results based on applying a multiplier of 5 for the hub weight, 4 for the risk and cost, and 3 for the drag and survivability.

In addition, copies of the hub concepts were given to BHTI experts in survivability, cost, weight, and drag for rating in their particular field of expertise only. These results are shown in Table V, along with a rating for the parts count. Again, weighted totals are also presented.

These ratings were not the sole basis for selection of the two hub concepts, since only preliminary layouts were made for each hub concept. The results of these ratings were used as a guide along with engineering judgement in the selection process.

Concept #2 was rated the highest by the experts (weighted and unweighted) and very high by the engineers (highest unweighted and second weighted) and was selected as one of the hub concepts to be refined. Concept #3 was rated next highest by the experts and third highest by the engineers; however, it was not selected because of its folding limitations and the compromises in the flap flexure due to the proximity of the attachment lugs. Concept #1 was selected as the other concept because, even though it showed the greatest risk, it has the least parts count, weight, and cost and had the highest weighted total by the engineers. Concept #6 was not selected; however, if additional flapping ability becomes necessary (which might be required for future testing on the RSRA), this concept could be the most attractive.

TABLE IV. ENGINEER'S HUB CONCEPT RATING

	Weighting Factor	Hub Concept 1	2	3	4	5	6	7	8
Survivability	(3)	3.94	5.94	6.35	4.00	5.83	6.67	6.11	5.39
Risk	(4)	3.33	7.28	6.12	4.17	6.44	7.22	8.39	7.56
Cost	(4)	7.00	6.61	5.88	6.61	5.67	5.50	5.67	5.72
Drag	(3)	7.44	6.72	7.29	7.50	6.11	6.44	4.83	4.39
Weight	(5)	8.50	7.17	6.53	8.28	4.83	6.06	5.06	4.33
Unweighted Total		30.21	33.72	32.17	30.56	28.88	31.89	30.06	27.39
Weighted Total		136	129	121	119	108	120	114	104

TABLE V. EXPERT HUB CONCEPT RATING

	Weighting Factor	Hub Concept							
		1	2	3	4	5	6	7	8
Survivability	(3)	2	5	5	4	5	5	4	3
Part Count	(4)	10	8	9	8	7	3	5	4
Cost	(4)	9	8	6	5	4	7	3	2
Drag	(3)	3	10	9	4	7	6	5	8
Weight	(5)	7	8	6	9	5	4	3	2
Unweighted Total		31	39	35	30	28	25	20	19
Weighted Total		126	149	132	121	105	93	74	67

5. CONCEPT REFINEMENT CONSIDERATIONS

The two selected concepts, the damperless design and the bearingless design with dampers, were refined to the point that their physical properties and characteristics could be determined and related to the ITR Hub Technical Goals of the appendix. This involved determining the flapping ability and means of providing stability for each hub. Also, the blade attachment and pitch change elements were established with the emphasis on minimizing hub drag.

Before discussing the development of the selected hub concepts, it is important to identify the characteristics of the composite materials that could be employed. Table VI presents some of the material properties and considerations for applicable composite materials. The values shown in the table are representative of the materials, once temperature, moisture, resin variations, manufacturing defects and data scatter are taken into consideration. The peak allowable tension stress (steady plus oscillatory) values rule out Kevlar as a hub material and show one of the desirable aspects of graphite. Another characteristic of graphite is that its shear modulus is close to that of fiberglass while its tension modulus is much greater. The desirable aspects of fiberglass are its ability to undergo large strains and very gradual failure modes.

In general, Kevlar is applicable to secondary structures and fairings where significant loads are not present. Fiberglass is applicable to highly loaded areas and when large stiffnesses are not required. Graphite is applicable for a design when maximum stiffness is of primary interest.

TABLE VI. MATERIAL CHARACTERISTICS

	Kevlar	Fiberglass	Graphite
Unidirectional Tension Modulus (psi)	11×10^6	7.3×10^6	21×10^6
Unidirectional Shear Modulus (psi)	0.28×10^6	0.88×10^6	0.91×10^6
Peak Allowable Tension Stress (psi)	30,000	50,000	160,000
Density (lb/in^3)	0.049	0.072	0.057
Major Advantage	Durability	Good failure mode	Stiffness-to-weight ratio
Major Consideration	Low compression, shear and fatigue strength	Stiffness-to-weight ratio	Poor failure mode
Application	Secondary structures	Strength designs	Stiffness designs

6. BEARINGLESS HUB WITH DAMPERS

The design philosophy for the bearingless hub with dampers was to have a low hub moment stiffness with as much flapping ability as possible. Once the flap flexure was established, the stiffnesses of the yoke, cuff, and dampers were determined for inplane frequency placement and maximum damping. The effort then centered on developing the geometry of the pitch change element to meet the desired stiffnesses and to transition it into the blade attachment.

6.1 FLAPPING

Fiberglass was chosen as the yoke material for this design because of the desire for low stiffness and maximum flapping ability. With the 80,000 pounds centrifugal force, a minimum of 3.2 square inches of continuous unidirectional fiberglass would be required to keep the steady axial stress at 25,000 pounds per square inch. The unidirectional fiberglass consists of belts of roving that must bypass the shear restraint and interleave with the belts from the adjacent arms in the center section. In the areas of interleaving, approximately 60 percent of the laminate thickness will be made up of crossply material placed between the belts for continuity in reacting drive torque. These considerations will determine a minimum thickness of the center section.

The center section thickness and flexure width are iterated to determine the best combination for minimum hub stiffness and width (for reduced size of the pitch change cuff). As the width decreases, the thickness increases; however, if the flexure becomes too wide, the planform of the center section becomes large, which also increases the hub moment stiffness. The center section that evolved is 2 inches thick with 11.5-inch-wide flexures. The fiberglass belts are 4 inches wide, allowing 3.5 inches for housing the shear restraint.

With the center section established, the effort concentrated on sculpturing the thickness distribution of the flap flexure for minimum fiber stress. A tension beam analysis, which accounts for the inertia forces due to rigid blade flapping at one per rev and the centrifugal force, was used to evaluate the flap flexure. A triangular airload distribution is applied in the analysis to generate 5 degrees of flapping. The analysis calculates the moment distribution for the flap flexure and the associated fiber stress distribution for the specified flapping angle. Interlaminar shear stresses are not calculated in this procedure because of the complexity of shear distributions inside the flexure and the anisotropic properties of the material. Chord and torsion loads are not included in the analysis. The stresses associated with the chord and torsion loads are generally very small in the flap flexure portion of the yoke. The analysis is coupled to an optimization routine that has the ability to vary the thickness distribution of the flap flexure to achieve a specified fiber stress level. The hub moment stiffness was not treated as a constraint in the optimization process. The optimization routine has the constraints of maintaining the area of the fiberglass belts and a core of crossply material in the center of the flexure for housing the shear restraint. There is a total of 16 belts for the entire yoke (8 belts per arm and 4 belts on each side of the shear restraint). The thickness distribution is varied by adding crossply material between the belts and core. Each belt is 0.10 inch thick and the core is 0.15 inch thick, dictating a minimum flexure thickness of 0.55 inch.

Figure 11 shows the flexure thickness distribution and the resulting oscillatory bending moments and fiber stresses for an initial assumption of the thickness distribution. The maximum oscillatory fiber stress is 35,000 psi, which is unacceptable. Figure 12 shows the resulting flexure thickness distribution when the allowable fiber stress was set at 30,000 psi. The stress distribution is irregular because this was an intermediate calculation. The stress distribution could have been made smoother at this stress level with small variations in the flexure thickness distribution. Figure 13 shows the best or optimum flexure that has an oscillatory fiber stress of 22,000 psi for 5 degrees of flapping. These figures show the trend of the optimization routine to transition to and maintain the minimum flexure thickness. However, if the thickness distribution is transitioned to the minimum value as close as possible to the center section (this would provide the lowest hub moment stiffness), the resulting fiber stresses will go up to 32,000 psi, as shown in Figure 14.

Figures 11 through 14 show the fiber stresses of the yoke outboard of the hub clamp plates beginning at station 6. The yoke center section reacts the hub moments through interlaminar shear. Detailed stress analyses are required to determine the magnitude of the interlaminar shear stresses because the hub shears are shared between the clamp plates and the yoke. Also, interlaminar shear stresses are influenced by Poisson's ratio effects between the unidirectional and crossply material, curvature of the belts, stress concentrations at the crossply drop-offs, and residual stresses in the belts from curing. Most of these characteristics can be determined with a finite element analysis in which each ply is represented. BHTI's experience has shown that the interlaminar shear stresses for composite hubs can be below the endurance limit (approximately 1500 psi).

The optimum flexure thickness distribution of Figure 13 represents a long thin flexure that will not carry the droop loads or limit the droop excursions. The BHTI criterion for static droop

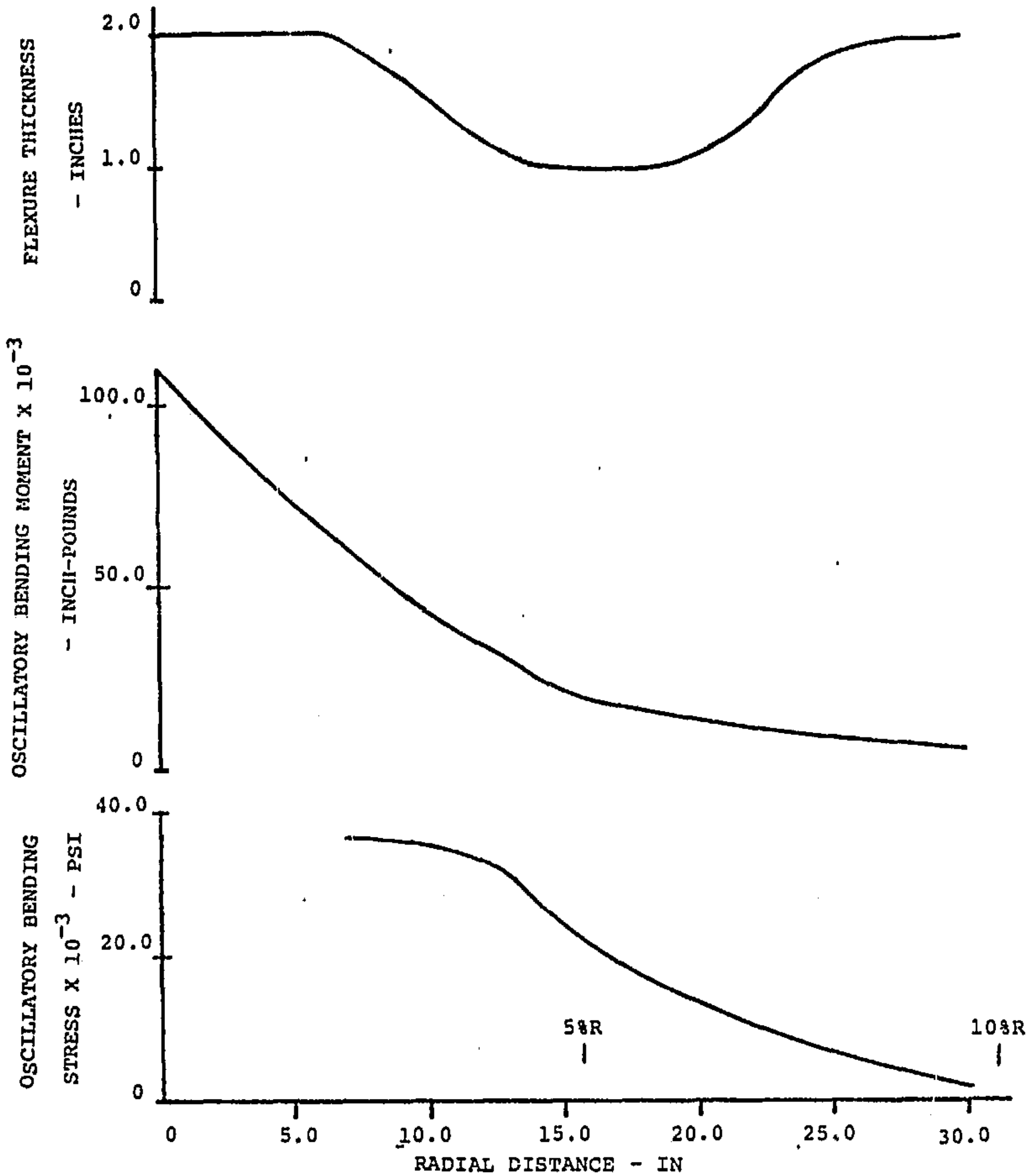

Figure 11. Tension Beam Analysis, 5 Degrees Flapping, Initial Assumption

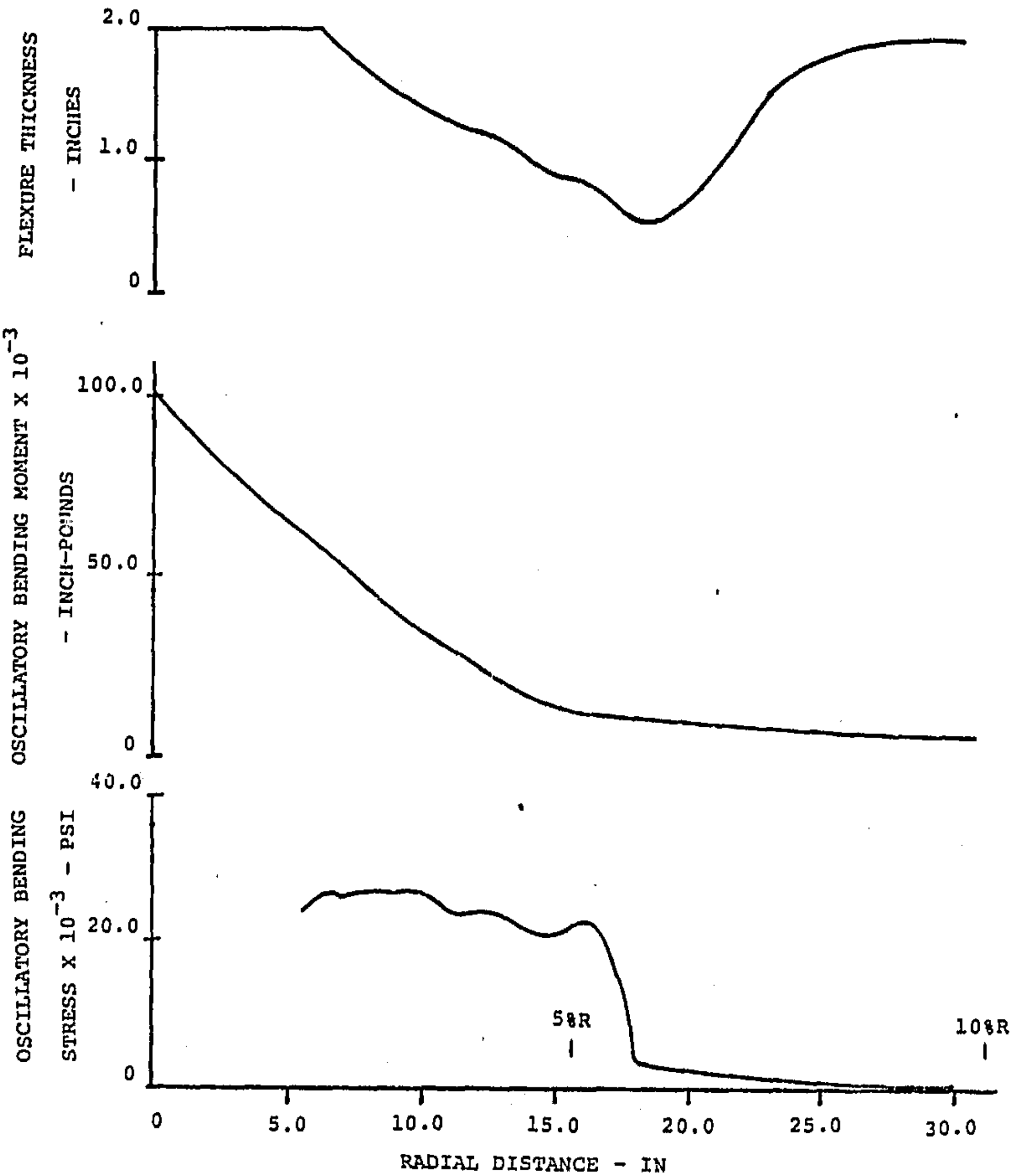

Figure 12. Tension Beam Analysis, 5 Degrees Flapping, Optimized for 30,000 psi Fiber Stress

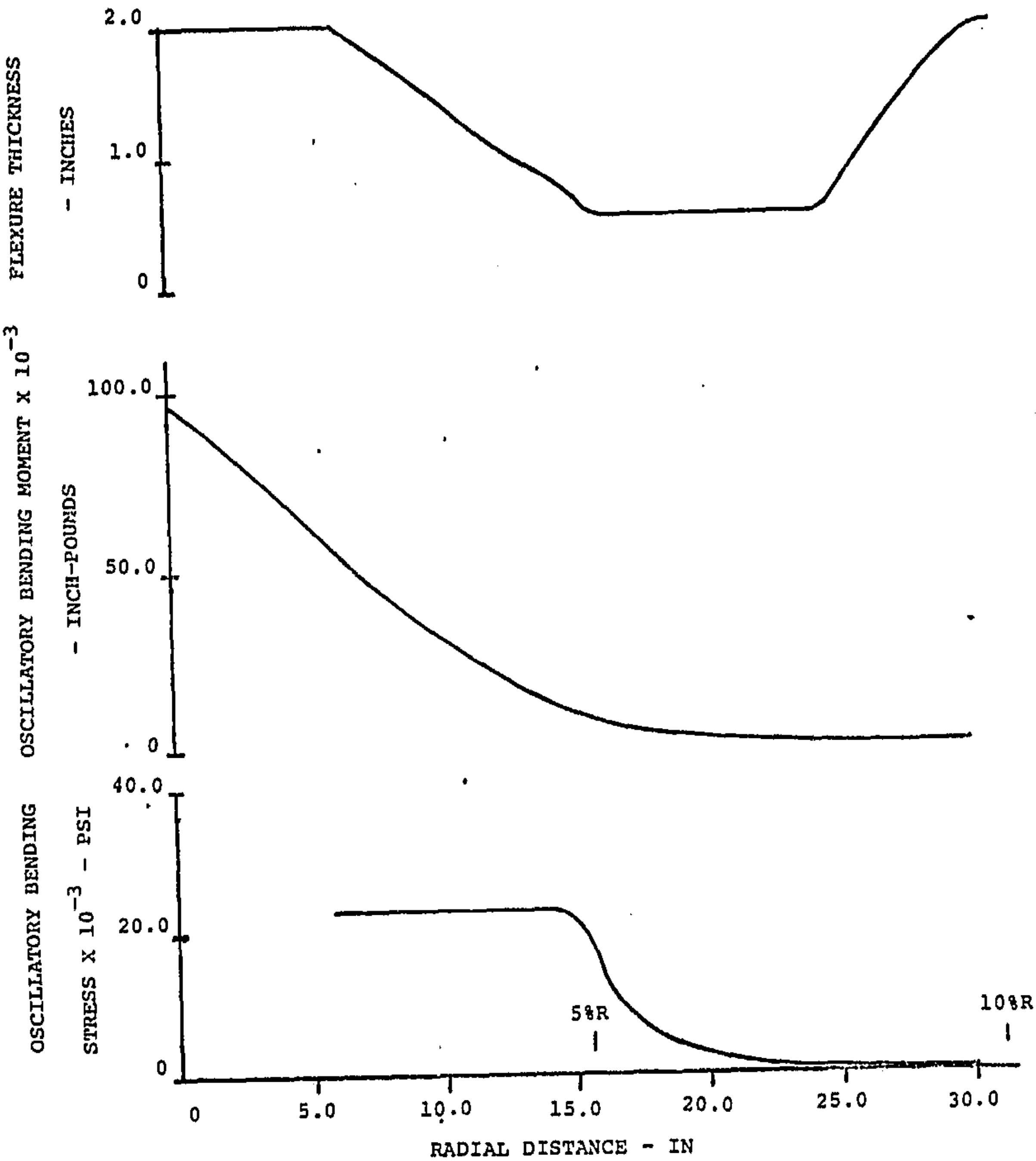

Figure 13. Tension Beam Analysis, 5 Degrees Flapping, Optimized for 22,000 psi

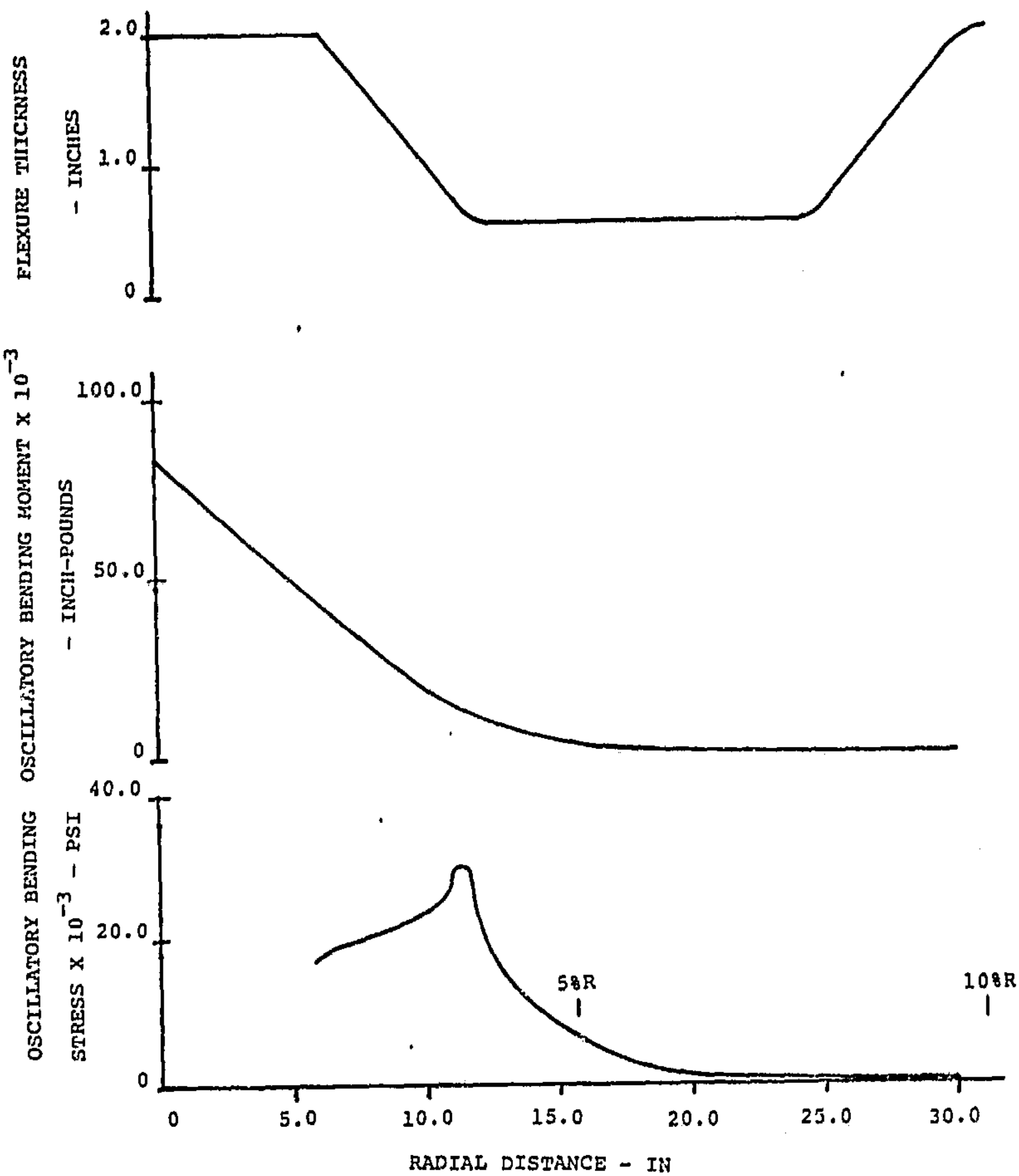

Figure 14. Tension Beam Analysis, 5 Degrees Flapping, Thinnest Possible Flexure

is that the flexure must have acceptable static stress for twice the blade weight with no interference between the blade and the tailboom. However, since this hub concept incorporates a cuff, a droop stop can easily be employed with extensions of the lower hub clamp plate and cuff. The cuff must be designed for the compression loads in the contact area of the droop stop. This can be accomplished without an increase in the parts count and with a very small weight penalty.

The resulting yoke beam stiffness distribution is shown in Figure 15.

The hub moment stiffness, as defined in the appendix, is 181,450 ft-lb/rad. If 18,000 psi fiber stress is assumed as an endurance limit for fiberglass, then the minimum rotor hub tilt angle is 3.96 degrees. This will result in a minimum rotor hub moment of 12,540 ft-lb. It should be noted that if a fail-safe approach instead of a safe-life approach is used in qualifying this hub, the minimum hub tilt angle would be increased to approximately 6 degrees. With the fiber stress distribution of Figure 13 for this hub, the fatigue life should exceed 10,000 hours once a flight spectrum is applied.

6.2 STABILITY

With the flapping flexure established, the effort concentrated on transitioning the flexure to an acceptable chordwise stiffness distribution for inplane frequency placement and damping with minimum torsional stiffness. This is done by narrowing the width as rapidly as possible while maintaining a constant area of unidirectional material. The narrow flexure will lower the torsional rigidity and maximize the efficiency of the damper. The Myklestad coupled natural frequency analysis was used in this process because of its ability to analyze the redundant yoke/cuff/damper assembly. This process involves placing the natural frequency at 0.7 per rev and maximizing the work that the damper performs. This dictates that the cuff inplane stiffness be as large as possible so it will not wash out the damper motion. Therefore, graphite was selected as the cuff material.

The elastic spring rate, K', of the damper is established with the cuff and yoke stiffness to provide the desired natural frequency. The resulting damping ratio is

$$C/C_c = \frac{K' \zeta^2 \gamma}{2 \, GI \, \omega^2}$$

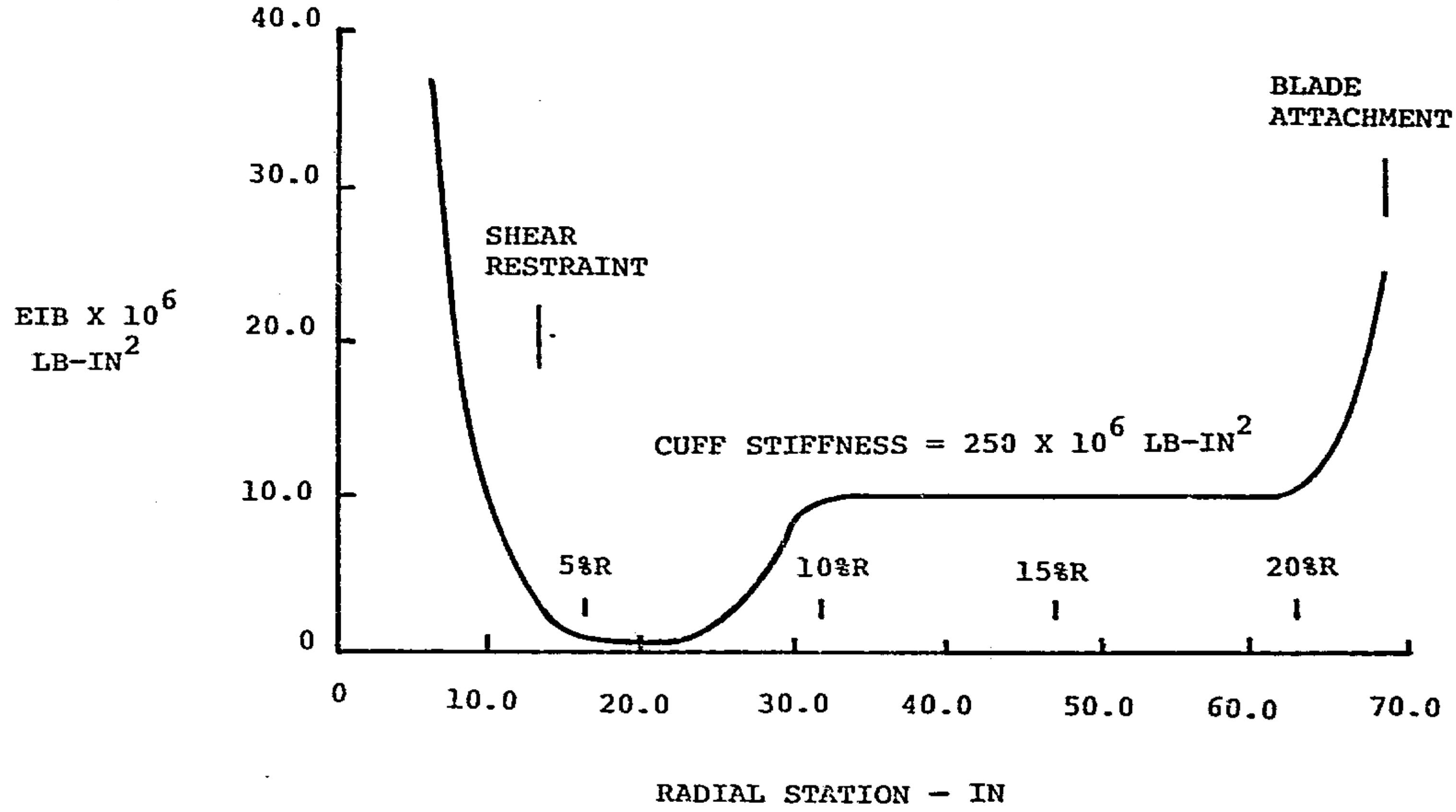

Figure 15. Yoke Beam Stiffness Distribution

where ζ is the damper displacement, GI is the generalized inertia, ω is the natural frequency, and γ is the loss tangent of the elastomeric damper. The loss tangent is the ratio of the damping spring rate of a material divided by its elastic spring rate. The amount of damping (lb/in-sec) that an elastomeric material will provide is equal to the damping spring rate (lb/in) divided by the frequency (rad/sec) at which the elastomeric material is cycled. Figure 16 shows the qualitative effects of the elastic spring rate on the natural frequency and damping ratio for a given yoke/cuff assembly. The figure shows that there is a maximum damper efficiency that can be achieved. Therefore, further increases in the damper elastic spring rate will result in a larger natural frequency and decreased damping ratio.

For this hub concept, an elastic spring rate of 2500 lb/in provided the maximum amount of damping (6 percent critical assuming a loss tangent of 0.65 for the elastomeric material, BTR VI). This involved placing the damper/shear restraint assembly as far inboard as possible (station 12.5) with the blade attachment at station 69. Figure 17 shows the resulting yoke chord stiffness distribution.

With the elastic spring rate of the damper established, the damper is then sized for acceptable fatigue life. The damper thickness, t, is determined by

$$t = \frac{\zeta}{\varepsilon} = \frac{0.19}{0.08} = 2.38 \text{ in}$$

where the displacement, ζ, is based on the expected motion for 0.6 degree lead-lag at 170 KTAS and the allowable strain, ε, is 8 percent.

The area, A, of the damper is determined by

$$A = \frac{t\,K'}{G'} = \frac{2.38\ (2500)}{180} = 33 \text{ in}^2$$

where G' is the elastic shear modulus of BTR IV at 8 percent strain. Since there are two dampers acting in parallel for each arm of the yoke (above and below the shear restraint) the area is divided between them. However, both must have the thickness of 2.38 inches. The resulting dampers have an outer diameter of 5.0 inches and an inner diameter of 1.5 inches.

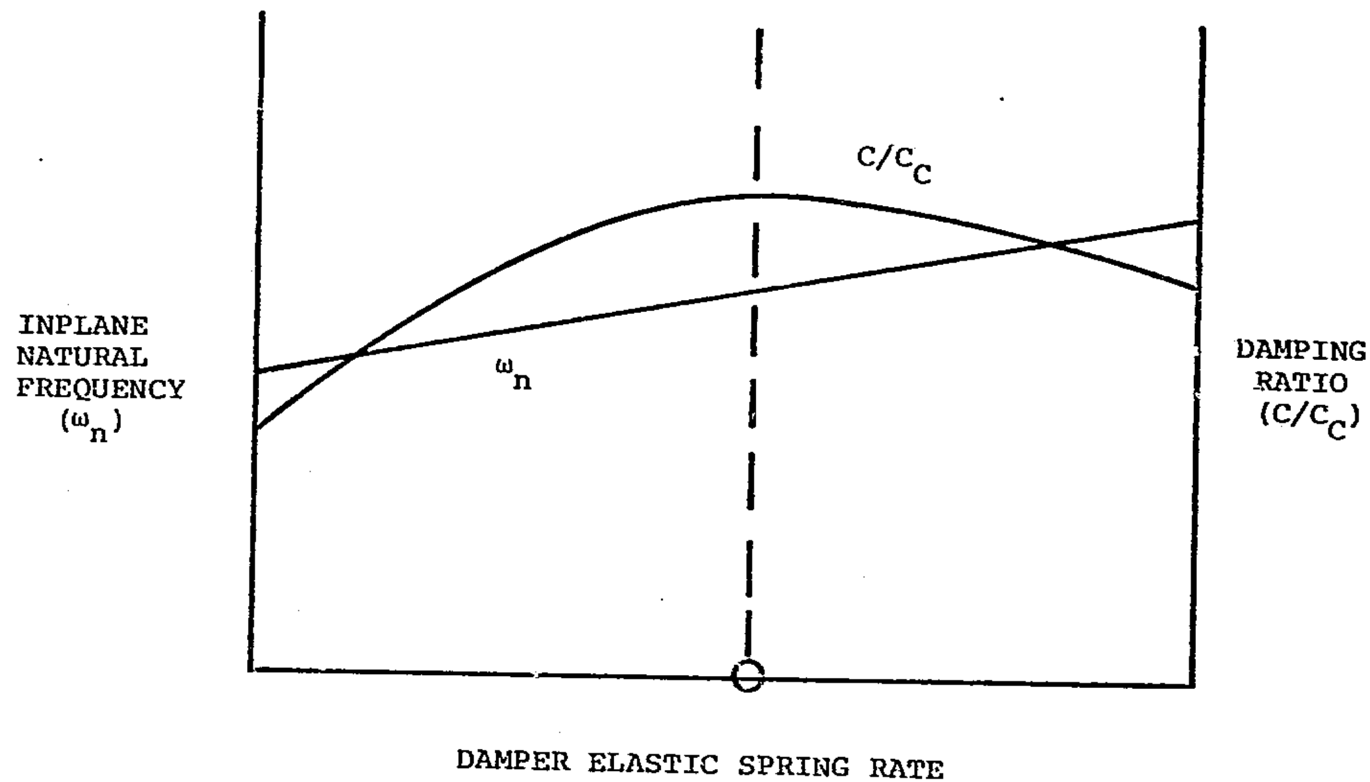

Figure 16. Effects of Damper Elastic Spring Rate on Natural Frequency and Damping Ratio

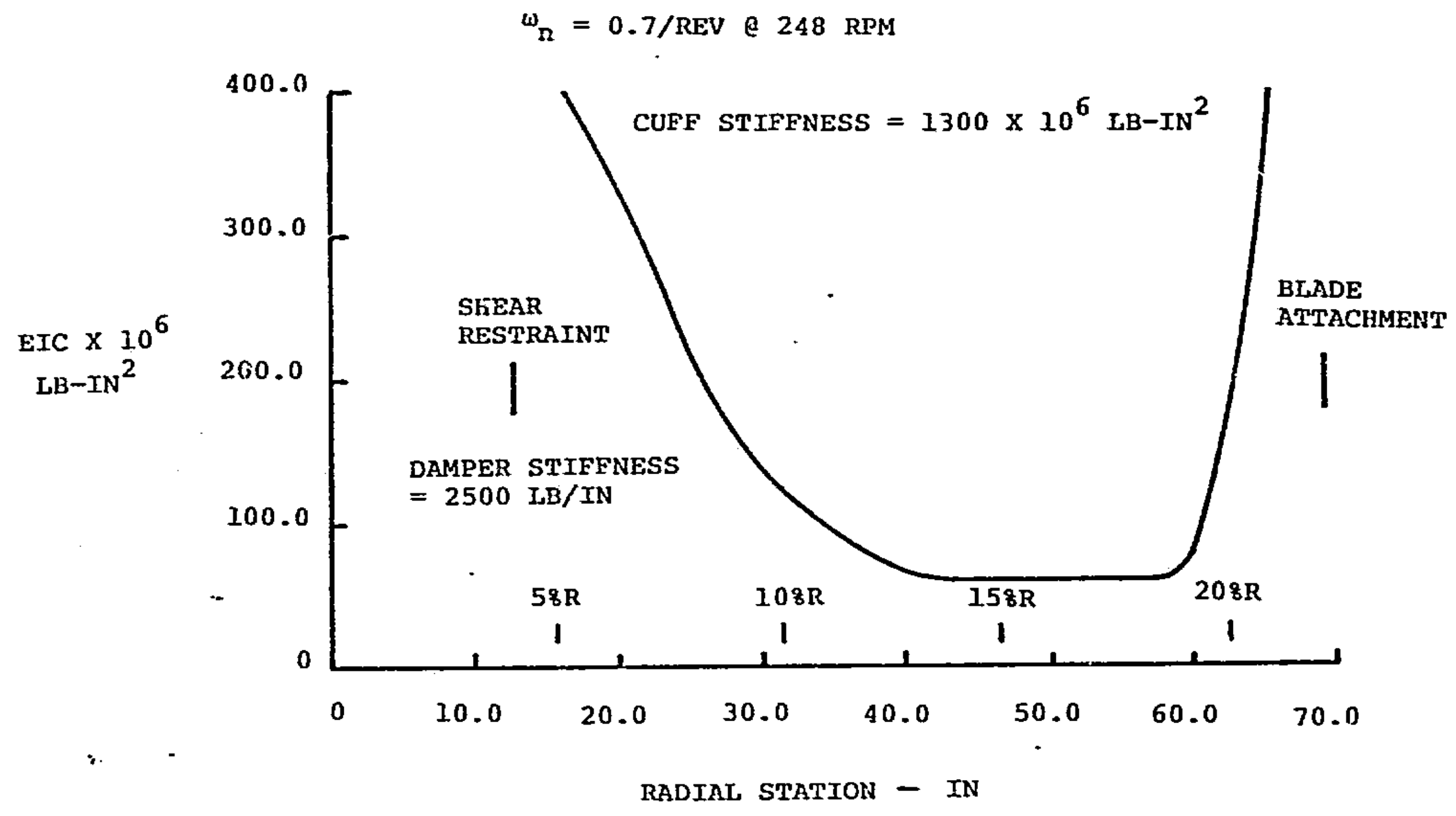

Figure 17. Yoke Chord Stiffness Distribution

The 6 percent critical damping at 0.7 per rev should provide an adequate stability margin for ground and air resonance for this hub concept. BHTI's experience during flight test of the Model 412 helicopter has shown that with one elastomeric damper inoperative, there is a negligible loss of stability.

6.3 BLADE ATTACHMENT

The design approach for the blade attachment lugs is to keep the thickness of the lugs as small as possible for minimum drag and the chordwise spacing as narrow as possible for easy transitioning from the yoke pitch change element. The yoke and cuff will share the beam and chord loads while the yoke carries all of the centrifugal force; but the attachment portion of the blade area must carry all of the beam, chord, and axial loads. Therefore, the lug sizing and spacing are determined by the requirements of blade attachment.

In determining the stresses in the material that forms the lugs, a series of stress concentration factors must be applied. One of these factors is based on the ratio of the total width of a lug, W, divided by the inner diameter, D. A high W/D ratio will provide a vertically compact lug, but it will have a high stress concentration factor. BHTI's experience and test data have shown that a W/D ratio of 1.6 is an acceptable configuration. This ratio implies a stress concentration factor of 2.3 that is applied to all loads. In addition, a stress concentration factor of 2.1 is applied to all steady loads and a factor of 1.65 is applied to all oscillatory loads. These factors are applied to the attachment loads of Table II and to the centrifugal force. The spacing, height, width, diameter, and area of the lug are iterated to determine the most compact attachment area that has a peak stress under 50,000 psi.

The resulting blade lug height is 4.3 inches with a width of 5.5 inches and an inner diameter of 3.3 inches. The centers of the lugs are 5.5 inches apart, providing an attachment area as compact as possible. This lug geometry was used for both hub designs in this program (reference Figures 20 and 25 introduced in Sections 6.6 and 7.5, respectively).

6.4 PITCH CHANGE

The considerations for the pitch change portion of the yoke are the transitions to the flap flexure and blade attachment, the area of the unidirectional material, and the requirement to maintain the desired chordwise stiffness. In addition, the configuration must provide as low a torsional stiffness as possible with acceptable shear stresses. The primary factors that affect the torsional stiffness are the shear rigidity, KG, and the centrifugal stiffening associated with the radius of gyration, $\bar{K}$. The torsional shear stresses, τ, are a function of the thicknesses of the walls, flanges, corners, and intersections. Table VII shows how well some candidate pitch-change area cross sections satisfy the above considerations.

Since the yoke of this hub concept required a tapered chordwise stiffness distribution that transitions to a moderate minimum value of 60 x 10^6 lb-in^2, the "triple H" cross-section was chosen as the geometry for the pitch change element. Another advantage of this cross section is its ability to tailor the stiffnesses independently. Figure 18 shows the geometry and properties of this section. The total yoke torsional stiffness is 210 in-lb/deg with the blade attachment at station 69 (22 percent radius) and the section of Figure 18 being used for the constant cross section of the yoke. The pitch change spring rate of elastomeric bearings that would be used in a conventional hub for a rotor this size was estimated to be 100 in-lb/deg. The centrifugal restoring moment for the ITR blades was estimated to be 280 in-lb/deg at 248 rpm. (This estimate is based on scaling from the Model 680 blades and rotor speed.) Therefore, the pitch control system force for the bearingless design would be 490 in-lb/deg compared to 380 in-lb/deg for the conventional hub. This is an increase of 29 percent.

6.5 DRAG

The primary drag considerations for the hub are the size and shape of the cuff and the blade attachment area. Clearance of the flap flexure for the ±24-degree pitch range and ±0.19-inch damper motion determines the minimum size of the inboard portion of the cuff. The thickness of the cuff was reduced, as the yoke size permitted, along the yoke for minimum frontal area. (This caused some manufacturing complications that are discussed in Section 9). The shape of the cuff is intended to reduce the download on the retreating side in high speed flight. Figure 19 demonstrates the means by which the download is further reduced by a small flow-separation strip. This approach was presented in NASA TN D-382,[1] but its effectiveness should be demonstrated by wind tunnel tests.

To reduce the drag of the blade attachment area, blade bolt fairings were incorporated. These fairings will reduce the drag by 50 percent; however, they will add four additional parts and must be removed when the blades are to be folded.

---

[1]Gessow, A., and Gustafson, F. B., Effect of Blade Cutout on Power Required by Helicopters Operating at High Tip-Speed Ratios, NASA TN D-382, September 1960.

TABLE VII. PITCH CHANGE ELEMENT CROSS SECTIONS

	Application	Characteristics
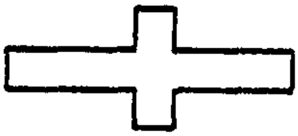 Cruciform	Low EIC Tailored Stiffnesses	High $\bar{K}$, τ Difficult Transitions
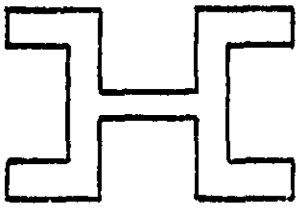 Back to Back C	High EIC Tailored Stiffnesses	Moderate $\bar{K}$ Low τ Good Transitions
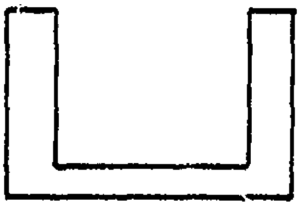 Channel	Shear Center Offset High EIC	High $\bar{K}$ Low τ Difficult Transitions Poor Tailoring
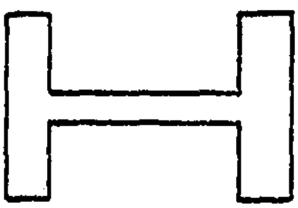 H	High EIC	High $\bar{K}$, τ Good Transitions Poor Tailoring
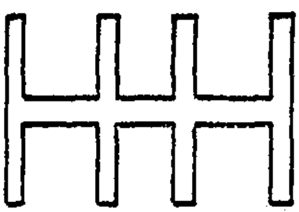 Triple H	Low to Moderate EIC Tailored Stiffnesses	Low $\bar{K}$, τ Good Transitions Independent Tailoring

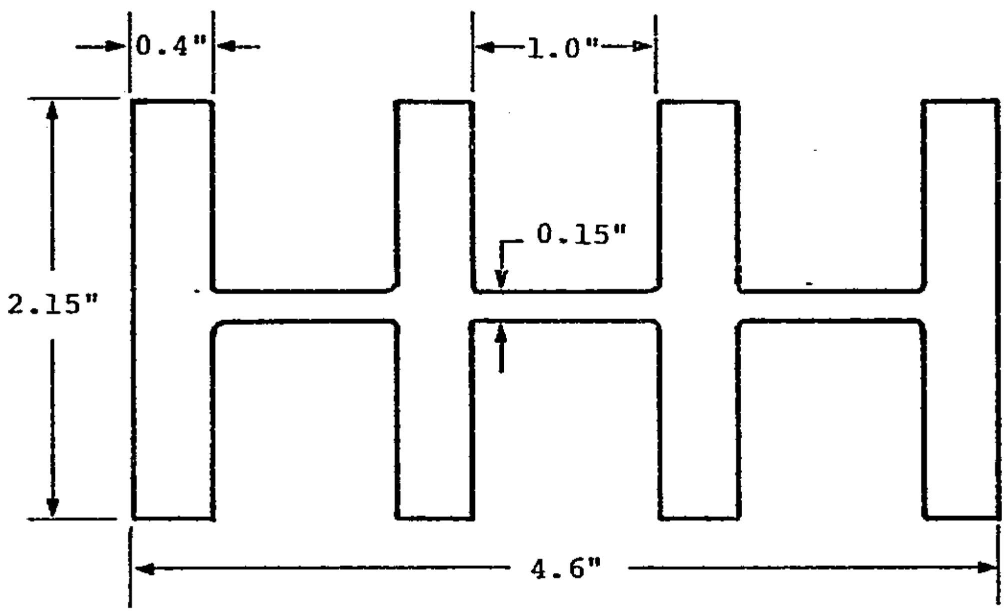

- EIB – 10×10^6 LB-IN^2
- EIC – 60×10^6 LB-IN^2
- SHEAR RIGIDITY – 135,270 LB-IN^2
- CENTRIFUGAL STIFFENING – 225,880 LB-IN^2 (80,000 LB CF)

Figure 18. "Triple H" Pitch Change Element Geometry

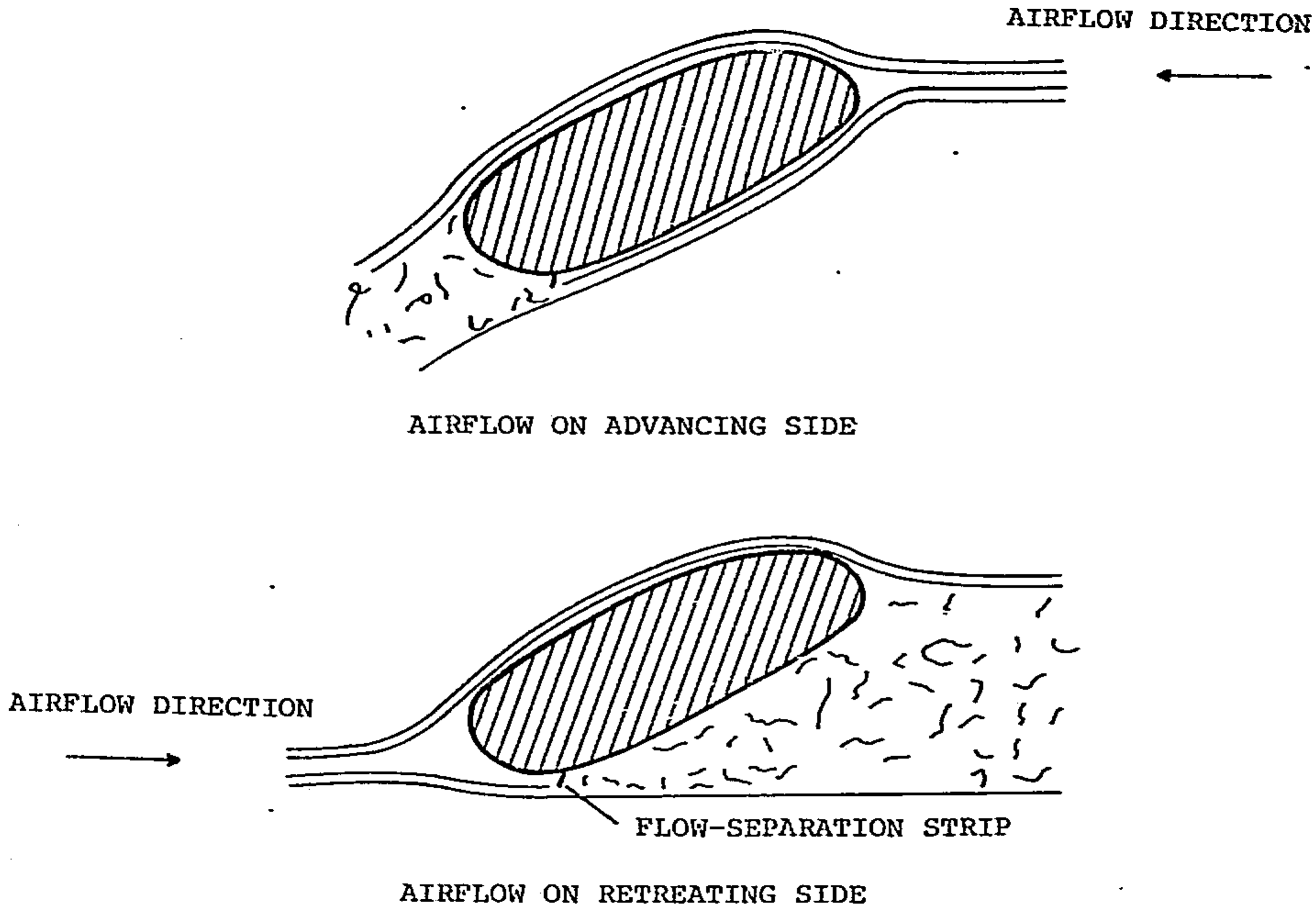

Figure 19. Cuff Shape for Reduced Download

Table VIII presents a breakdown of the radial extent, frontal areas, drag coefficients and flat plate drag areas for this hub concept. The values for the areas represent two arms of the hub. The center section consists of the clamp plates, yoke flap flexure, and inboard portion of the cuff where the average drag coefficient would be approximately 0.5. The cuff values represent the streamline portion of the hub where the drag coefficient would be approximately 0.2. The blade attachment values represent the entire lug area and include the effect of the blade bolt fairings that will lower the drag coefficient to approximately 0.25. The main rotor mast and pitch links are not included in the drag area. The resulting total flat plate drag is 2.43 ft^2 compared to the ITR goal of 2.8 ft^2.

TABLE VIII. DRAG OF BEARINGLESS HUB WITH DAMPERS

Hub Component	Radial Extent (ft)	Area (ft^2)	Drag Coefficient	Flat Plate Area (ft^2)
Center Section	1.8	2.69	0.5	1.35
Cuffs	3.8	4.75	0.2	0.95
Blade Attachments	0.6	0.52	0.25	0.13
Total		7.96		2.43

6.6 PARTS COUNT

Figure 20 shows the refined configuration of the bearingless hub with dampers. The major components are identified on the sketch. Table IX shows the parts count for this hub concept. These parts represent the nonstandard parts that would be identified on the rotor hub installation drawing. There are eight individual dampers in this hub; however, the dampers would be supplied in sets of two for each arm of the yoke. The upper and lower cone sets (not shown on sketch) are also two pieces each but are supplied as two sets. The parts count is 38 for this hub compared to the ITR goal of 50 parts.

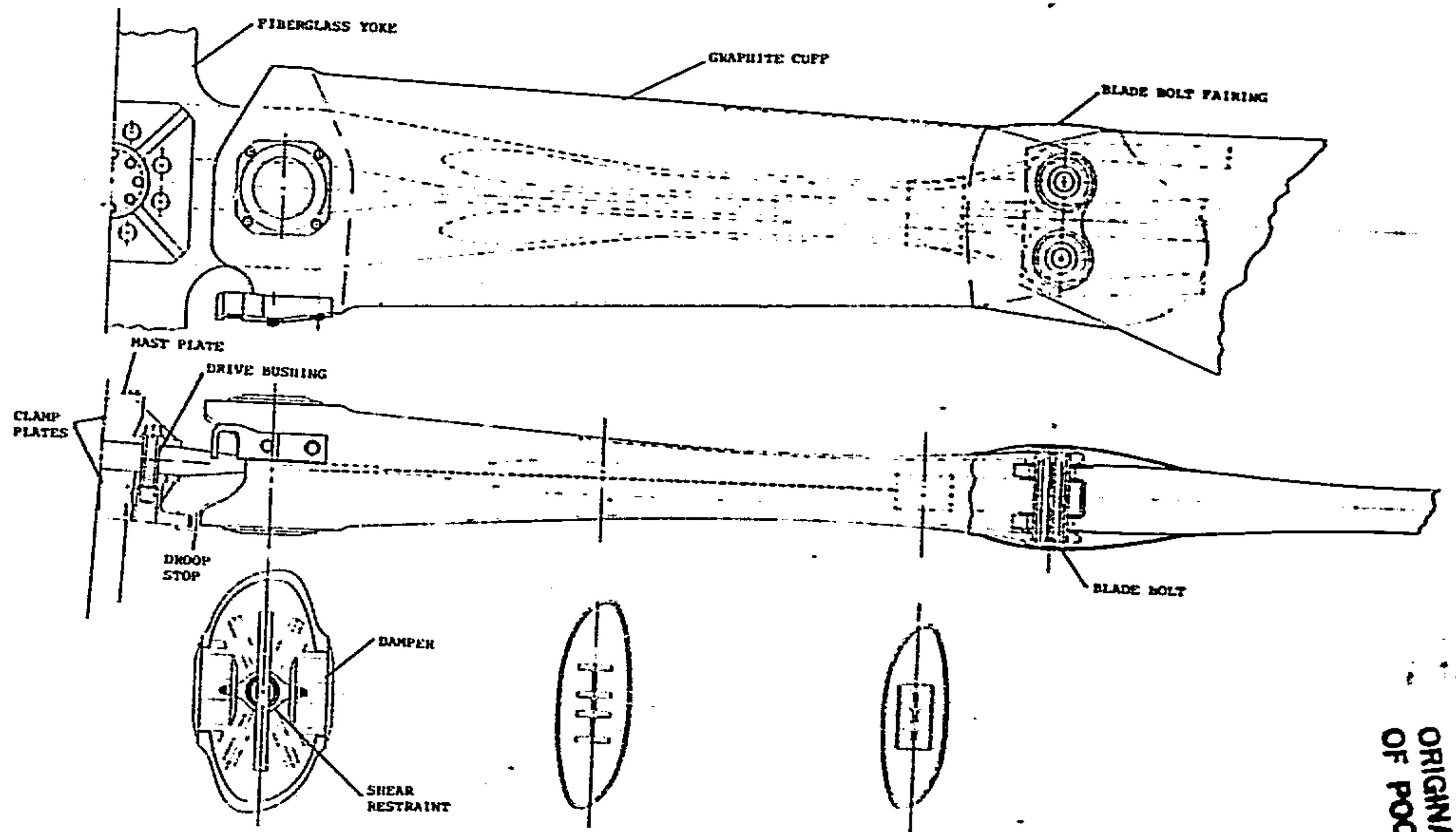

Figure 20. Bearingless Hub With Dampers

TABLE IX. PARTS COUNT OF BEARINGLESS HUB WITH DAMPERS

Part	Number
Yoke	1
Cuff	4
Damper Set	4
Shear Restraint	4
Clamp Plate	2
Mast Plate	1
Drive Bushing	8
Cone Set	2
Blade Bolt	8
Blade Bolt Fairing	4
Total	38

6.7 WEIGHT

A weight breakdown is presented in Table X. The volumes of the yokes and cuffs were determined and the appropriate densities of fiberglass and graphite (see Table VI) were applied. To keep the weight of the hub as low as possible, titanium (density of 0.16 lb/in^3) was used for all of the metal parts. The weight of the dampers and shear restraints was estimated based on similar BHTI designs. The total weight of this hub is 400.6 pounds compared to the ITR goal of 400 pounds.

TABLE X. WEIGHT OF BEARINGLESS HUB WITH DAMPERS

Component	Weight (lb)
Yoke	137.8
Cuffs	132.0
Clamp Plates, Bolts, Bushings, Pitch Horns	34.2
Blade Bolts, Bushings	48.6
Dampers	32.0
Shear Restraints	16.0
Total	400.6

7. BEARINGLESS HUB WITHOUT DAMPERS

The design philosophy for the bearingless hub without dampers is to provide aeroelastic couplings for stability without complex and bulky joints at the center section or the blade attachment areas. The emphasis of this design is to keep the hub moment stiffness, drag, and torsional stiffness as low as possible. Since detailed aeroelastic stability analyses would be required to determine the magnitude and effectiveness of the couplings, and such analyses were ruled out for this study, the effort of this program concentrated on mechanisms for achieving the couplings.

7.1 STABILITY

Stability is the obvious key for this hub concept; therefore, it was addressed first. Boeing Vertol's experience with the bearingless main rotor (BMR) has shown that the flap-lag coupling associated with the pretwist of the flexbeam and lag-torsion coupling, together with the hub moment stiffness, can produce stabilizing effects.[2]

To achieve the desired pitch-lag coupling (increased pitch with lag), the first attempts were to use a "channel" pitch change element geometry (see Table VII). This geometry has an offset shear center that could produce some pitch-lag coupling. However, it is very difficult to transition the fibers from the flexure into this geometry. The fibers must undergo a significant amount of transformation to achieve the "channel." The fibers must form the web as well as the flanges of the cross section to provide the shear center offset. This is very difficult to transition into lugs for blade attachment. Also, if the channel has sufficient chordwise stiffness for proper natural frequency placement, the resulting torsional stiffness, due to the large radius of gyration, would have been unacceptable. Therefore, the attempt to provide pitch-lag coupling by the structure of the pitch change element was discontinued.

Some amount of pitch-lag coupling can be achieved by canting the pitch links. But the diameter of the swashplate must be larger than the radial position of the pitch horn attachment to achieve the desired pitch-lag coupling. Other means of inducing this coupling are through negative droop at the blade attachment and

---

[2]Design, Development and Flight Demonstration of the Loads and Stability Characteristics of a Bearingless Main Rotor, Boeing Vertol; USAAVRADCOM-TR-80-D-3, June 1980.

indirectly through the combination of flap-lag and pitch-flap couplings that are present in the design. For this concept, negative droop is not incorporated at this time because of the unfavorable moments it induces in the yoke, but it could be accommodated should a detailed stability analysis dictate that it is necessary. Previous BHTI investigations of the effects of kinematic couplings on rotor stability have disclosed that, for at least some hub configurations, the amount of thrust being produced by the rotor greatly affects the stabilizing ability of the couplings, even to the point of reversal of the stabilizing effects. These investigations have also shown that stabilization of both a "rigid" hub and a flexible pylon arrangement simultaneously by kinematic couplings may be difficult.

During the study of FRR variations for the bearingless hub with dampers, a mechanism involving a series of linkages in conjunction with a torque tube was devised. This mechanism can produce a significant amount of pitch-lag coupling and could be applied to the damperless hub configuration if needed. It is discussed in Section 10.2.2.

The most effective way to introduce the desired flap-lag coupling (flap up with lag) is to pretwist the yoke (as was done in the BMR), but this requires a complex center section and mast attachment. Transitioning the yoke from zero twist in the center section to maximum twist at the blade attachment is the simplest design, but the desired coupling will be washed out, especially with a low hub moment stiffness. The design approach taken was to transition the fibers from a flat inplane orientation in the center section to the desired pitch change element geometry with a twist of 15 degrees as rapidly as possible. The difficulty in this transition is a function of the flexure width and pitch change element geometry. The fibers must follow paths which are difficult to achieve by pushing filament-wound straps into place. The concave bending of fibers should be kept to a minimum to avoid wrinkles, which significantly reduce the strength of the structure.

The difficulties of twisting the yoke led to the decision for a split shear restraint and cuff arrangement. The split shear restraint is bonded to the upper and lower surfaces of the yoke, allowing the yoke to be narrower and deleting the need for cross-ply material in the flexure area.

The cuff is made of biased-ply fiberglass for high torsional stiffness to prevent blade pitch washout while having a relatively low inplane stiffness so that it will not interfere with the couplings of the yoke. The cuff also greatly improves the drag of the hub compared to a design with a torque tube.

Graphite was selected as the material for the yoke. This provides for an even narrower yoke and center section, which facilitates the twisting of the fibers. The graphite yoke will also reduce the radius of gyration in the pitch change element, significantly reducing the torsional stiffness of the yoke.

The resulting yoke is 9 inches wide just outboard of the center section, which is 2 inches thick. The flexure begins at station 5 (5 inches outboard of the rotor centerline) and transitions to a twist of 15 degrees at station 15 where the width is tapered to 7 inches and the thickness is 1 inch. The yoke chord stiffness at station 5 is 1500 x 10^6 lb-in^2, tapering rapidly to 200 x 10^6 lb-in^2 just outboard of station 15 where the yoke transitions to the pitch change element (see Section 7.3). The yoke chord stiffness distribution is shown in Figure 21.

7.2 FLAPPING

This yoke is stiffness designed for stability. That is, the beam ar chord stiffness distributions were established to provide the flap-lag coupling and inplane natural frequency placement. Attempts were made to provide as low a hub moment stiffness as possible. However, if the beam stiffness were reduced inboard of the flexure twist region, the flap-lag coupling would be washed out; and if the beam stiffness were reduced outboard of the flexure twist region, the inplane natural frequency would be compromised. Also, the beamwise contribution of the chord stiffness associated with twist contributes to the relatively high hub moment stiffness.

The center section thickness of 2 inches will provide for the interleaving of unidirectional material from the adjacent arms of the yoke and the buildup of crossply material for continuity in reacting drive torque. The minimum section, 7 inches wide and 1 inch thick, has a droop stress of 39,045 psi for 1g (based on droop moment of Table I). This provides a very large margin of safety when compared to an allowable stress of 160,000 psi for graphite in compression. The stress distribution based on the tension beam analysis is shown in Figure 22. The resulting oscillatory fiber stress for 5 degrees of flapping is 69,800 psi. There is very little flexure fatigue data for graphite, but an acceptable allowable stress would be 75,000 psi, once environmental and manufacturing effects are included. The yoke beam stiffness distribution is shown in Figure 23.

The hub moment stiffness is 336,660 ft-lb/rad. This is significantly higher than the technical goal; but as stated above, this is the minimum value that would provide the flap-lag coupling and inplane natural frequency placement. The minimum hub tilt angle is 5.37 degrees, based on 75,000 psi as an endurance limit. This

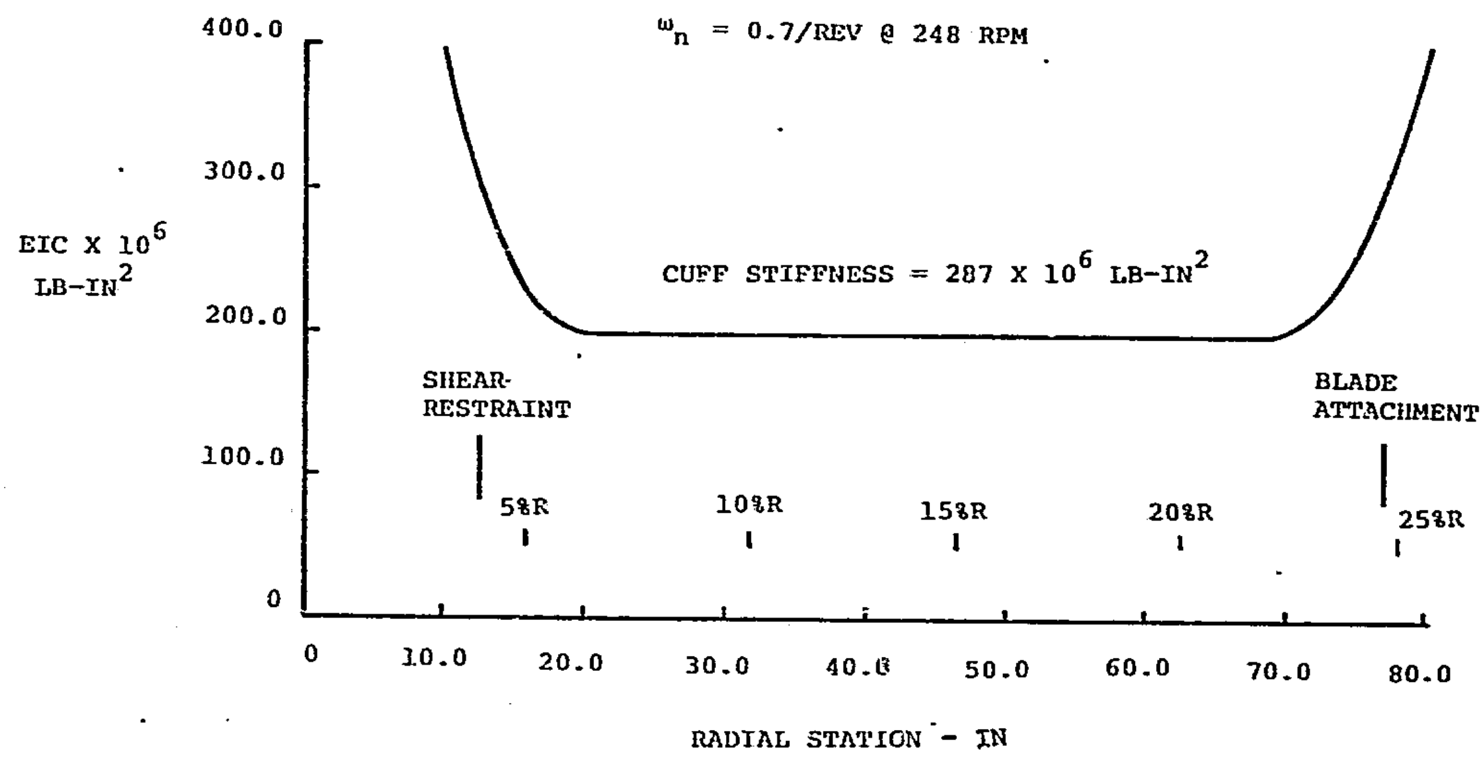

Figure 21. Yoke Chord Stiffness Distribution

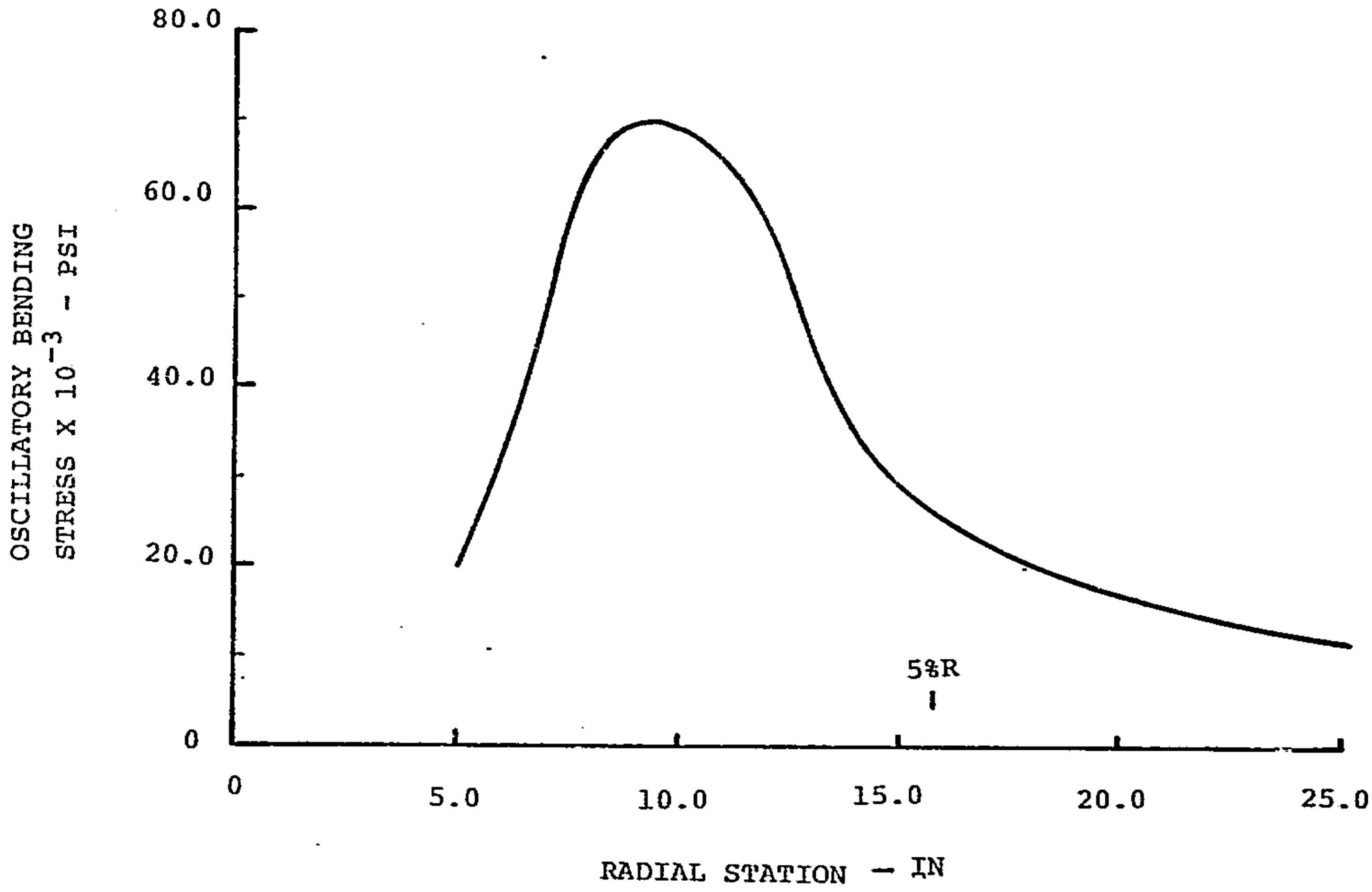

Figure 22. Tension Beam Analysis, 5 Degrees Flapping, Fiber Stress Distribution

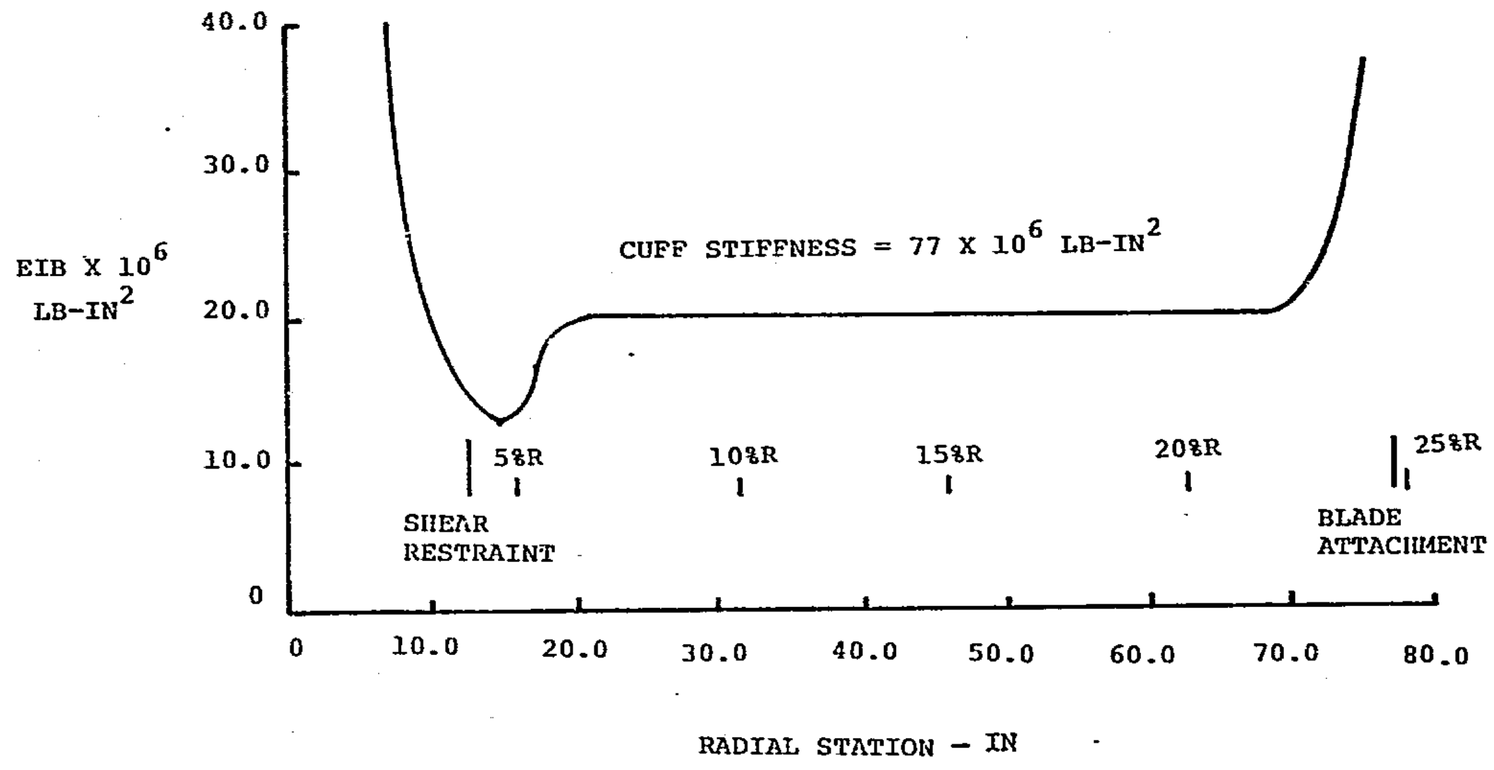

Figure 23. Yoke Beam Stiffness Distribution

sets the minimum hub moment at 31,551 ft-lb. Since the fiber stress is less than the endurance limit, this yoke should have a fatigue life of over 10,000 hours.

7.3 PITCH CHANGE

The considerations for the pitch change portion of the yoke are the same as those discussed in Section 6.4. These are the transitions to the flap flexure and the blade attachment, the required area of the unidirectional material, and maintenance of the desired chordwise stiffness while providing as low a torsional stiffness as possible with acceptable shear stresses.

Since this yoke requires a relatively high chordwise stiffness for natural frequency placement (200×10^6 lb-in^2), the "back-to-back C" cross section was chosen as the geometry for the pitch change element (see Table VII). This cross section has the ability to provide the required chordwise stiffness with a moderate amount of centrifugal stiffening compared to the "H" cross section. Figure 24 shows the geometry and properties of the selected cross section. The use of graphite in this yoke helps keep the centrifugal stiffening to a minimum. The flanges of this cross section contain all of the unidirectional material (3.2 in^2). The vertical walls and horizontal web are made of graphite fabric for stabilizing the structure.

The blade attachment for this design was moved outboard to station 78 (25 percent radius). The cross-section geometry is maintained for 48 inches (station 20 to 68). This results in a total yoke spring rate of 290 in-lb/deg. Therefore, the pitch control system force for this design (blades included) would be 570 in-lb/deg compared to 380 in-lb/deg for the conventional elastomeric hub. This is an increase of 50 percent.

7.4 DRAG

The drag considerations for this hub design are the same as those discussed in section 6.5. The addition of the cuff for the damperless hub significantly reduces the drag. The narrow flexure width (due to the use of graphite) minimizes the size of the inboard portion of the cuff for flap flexure clearance. The cuff was shaped for reducing the download on the retreating side at high speed flight, similar to the cuff shape of the other design. The cuff of the damperless design extends to 25 percent radius (for torsional stiffness considerations), compared to 22 percent for the other design. Blade bolt fairings are also included in the damperless design to reduce the drag coefficient of the blade attachment area. Table XI presents a breakdown of the radial extent, frontal areas, drag coefficients, and flat plate drag

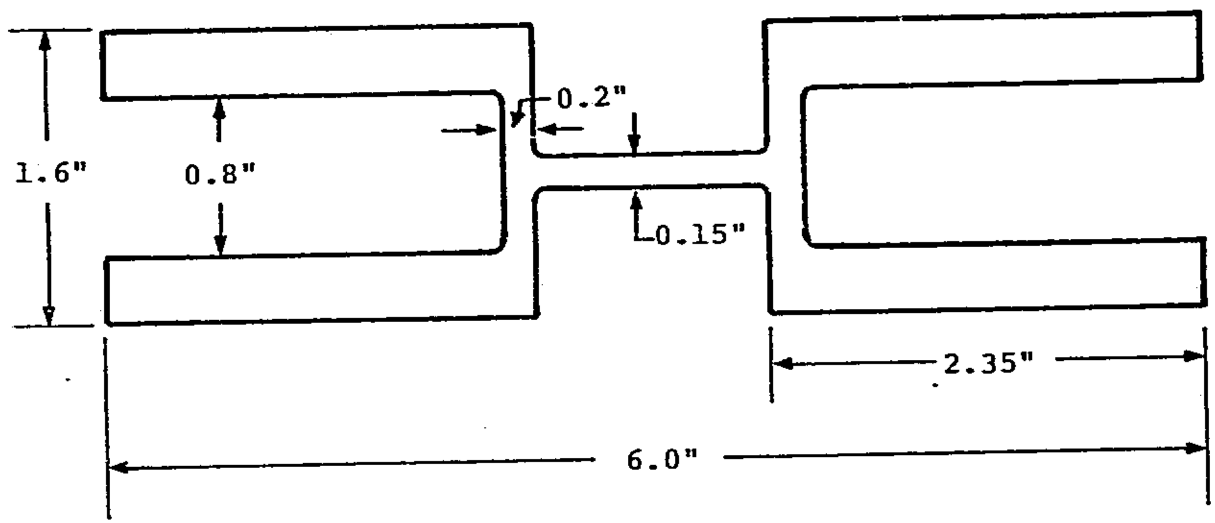

• EIB	– $20X10^6$ $LB\text{-}IN^2$	
• EIC	– $200X10^6$ $LB\text{-}IN^2$	
• SHEAR RIGIDITY	– 187,800 $LB\text{-}IN^2$	
• CENTRIFUGAL STIFFENING	– 610,590 $LB\text{-}IN^2$	(80,000 LB CF)

Figure 24. "Back-to-Back C" Pitch Change Element Geometry

areas for this hub concept. These parameters are discussed in Section 6.5. The resulting flat plate drag is 2.31 ft^2 compared to the ITR goal of 2.8 ft^2.

TABLE XI. DRAG OF BEARINGLESS/DAMPERLESS HUB

Hub Component	Radial Extent (ft)	Area (ft^2)	Drag Coefficient	Flat Plate Area (ft^2)
Center Section	1.31	1.96	0.5	0.98
Cuffs	4.9	5.98	0.2	1.20
Blade Attachments	0.6	0.52	0.25	0.13
Total		8.46		2.31

7.5 PARTS COUNT

Figure 25 shows the refined configuration of the bearingless damperless hub. The major components are identified on the sketch. Table XII shows the parts count for this hub concept. These parts also include the nonstandard parts that would be identified on the rotor hub installation drawing. There are eight individual shear restraints in this hub; however, they would be supplied in sets of two per arm of the yoke. The parts count is 34 for this hub compared to the ITR goal of 50.

TABLE XII. PARTS COUNT OF BEARINGLESS/DAMPERLESS HUB

Part	Number
Yoke	1
Cuff	4
Shear Restraint Set	4
Clamp Plate	2
Mast Plate	1
Drive Bushing	8
Cone Set	2
Blade Bolt	8
Blade Bolt Fairing	4
Total	34

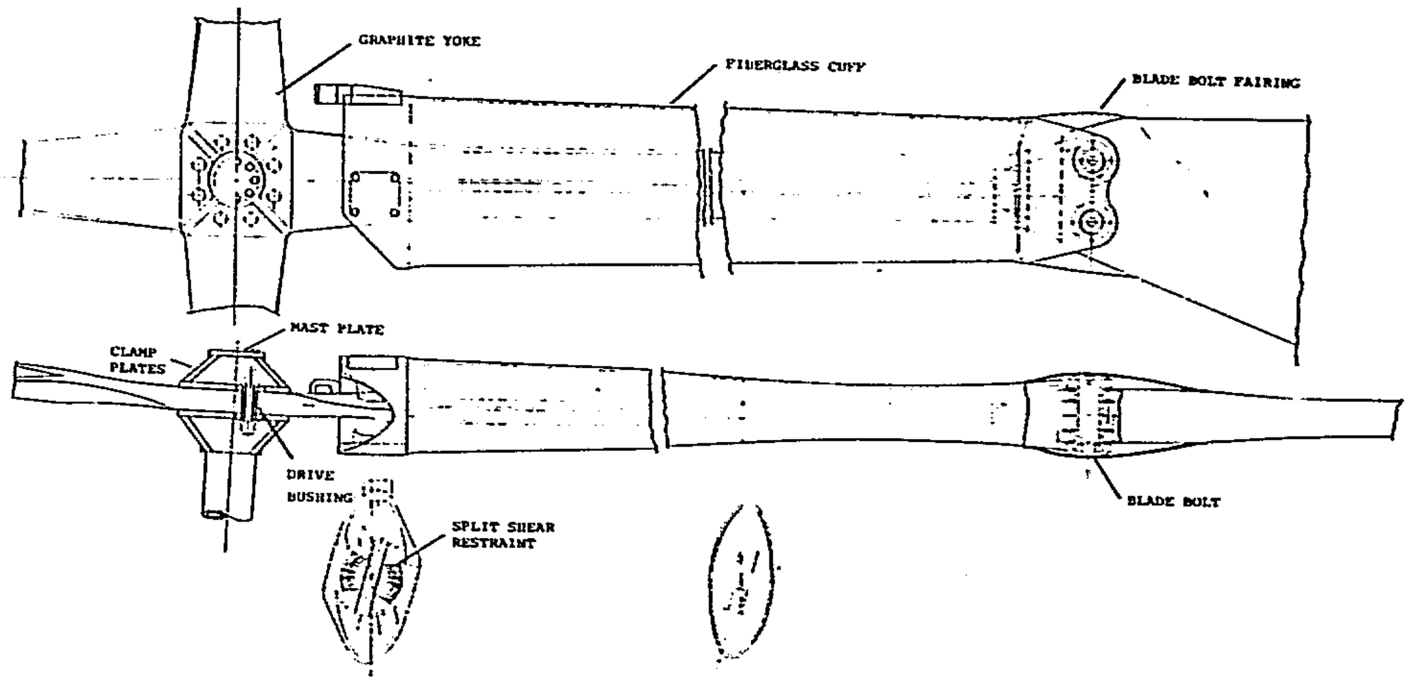

Figure 25. Bearingless Hub Without Dampers

7.6 WEIGHT

A weight breakdown is presented in Table XIII. The volumes of the graphite yoke and fiberglass cuffs were determined and the appropriate densities from Table VI were applied. As in the bearingless hub with dampers, titanium was used for all of the metal parts. The clamp plates would be several pounds lighter for the damperless hub because the center section is smaller and they do not need to extend to form a droop stop. However, the clamp plates must be thicker to withstand the larger hub moments. The shear restraint weights include an estimate of the hardware necessary to house them to the cuffs. The total weight of this hub is 385.82 pounds compared to the ITR goal of 400.0 pounds.

TABLE XIII. WEIGHT OF BEARINGLESS/ DAMPERLESS HUB

Component	Weight (lb)
Yoke	106.4
Cuffs	167.2
Clamp Plates, Bolts, Bushings, Pitch Horns	31.6
Blade Bolts, Bushings	48.6
Shear Restraints	32.0
Total	385.8

8. MERIT FUNCTION

The physical properties of both hub concepts have been identified for determining their merit factors according to the procedure in the appendix. The weight and drag values for each hub included the hub portions of the blade attachment area. Since the damperless hub extends 9 inches farther than the other hub, its weight and drag are representative of a larger percentage of the rotor radius (25 percent compared to 22 percent). In a more rigorous trade-off evaluation of weight and drag, the entire rotor systems must be compared. The remaining parameters are discussed in the following paragraphs.

The vulnerability of a hub is a function of the vulnerable area and probability of kill based on the most severe threat. A 23-mm HEI projectile with a super-quick fuse would have approximately a 4-inch cutting width in the cuffs of both hub configurations. A 23-mm HEI projectile with a delayed fuse will cut a smaller hole in the cuffs but would produce a severe internal blast due to the confined volume inside the cuffs. The delayed fusing that does not pass through the cuffs presents the greatest threat to the bearingless hub concepts because the load-carrying yoke is at the center of the cuffs. Both hub concepts present a significant amount of vulnerable area, which reduces their survivability. For the damperless hub configuration, the probability of surviving a hit with a delayed-fuse round is estimated to be 0.3. The bearingless hub with dampers was assigned a reduced value of 0.25 because of its larger internal volume, which will tend to magnify the blast, and its smaller yoke cross section.

The bearingless hub with dampers will have a very high probability that the rotor will be free from air/ground resonance. BHTI's experience has shown that there is very little loss of stability with one damper out on this type of hub design. Therefore, the probability that the rotor system will be stable is 0.9998. The damperless hub configuration should be stable for many flight conditions (as was the BMR). However, there will be instances where combinations of the rotor thrust and airframe dynamics could possibly result in instabilities. Therefore, the probability that the damperless hub will be stable was set at 0.9.

The composite parts for the hub configurations will have a high probability of exceeding an MTBR of 3000 hours because of their stress levels. Even though the metal parts are made of titanium, BHTI's experience has shown that they would also exceed an MTBR of 3000 hours. There is very little high cycle fatigue data for the elastomeric pivot bearings used for the shear restraints in both hub configurations. Therefore, the probability of each shear restraint having an MTBR of 3000 hours is set at 0.95. The damperless hub has 30 composite and metal parts and 4 shear restraints, so the probability, P_R, of exceeding the reliability goal is

$$P_R = (0.9998)^{30} (0.95)^4 = 0.8096$$

The bearingless hub with dampers has four elastomeric dampers that were sized for 0.08 in/in strain at V_H. There is also a limited amount of high cycle fatigue data for high loss tangent elastomeric material. However, once a flight spectrum is applied, there is a good probability that the MTBR of 3000 hours would be exceeded. Therefore, the probability for each damper set was established to be 0.99. The probability of the bearingless hub with dampers exceeding the reliability goal is

$$P_R = (0.9998)^{30} (0.95)^4 (0.99)^4 = 0.7777$$

The hub configurations are very similar from a manufacturing point of view. They involve the winding and interleaving of belts for their yokes and helical winding for the cuffs. They would have similar material costs and quality control requirements. Therefore, both hub configurations would be rated the same for manufacturing costs. The labor involved in the layup and curing of bearingless rotor hubs is a function of the production rate. The machining costs would be similar to conventional rotor hubs; therefore, a qualitative rating of 5 is given to each hub configuration.

The bearingless hub with dampers is designed for maximum damper efficiency. The addition of damper strips to the yoke would interfere with the ability of the existing dampers. Therefore, it is not practical to add additional damping to this design. Damper strips could be added to the damperless hub with little interference in the functions of the hub. The amount of work that the damper strips could perform is a function of the contribution that the elastic spring rate of the damper strips makes to the natural frequency of the rotor system, so there is a limited practicality to incorporating an effective amount of auxiliary damping to the damperless hub configuration.

Once the effects of the centrifugal restoring moments of the blades are considered, the pitch control system forces for both hub configurations will not exceed 1.5 times the forces of a conventional rotor system.

Table XIV presents the merit factors and merit functions for both hub configurations. The merit functions were calculated two times - once with the established vulnerability merit factor and once with a value of 1.0.

TABLE XIV. MERIT FUNCTION

Merit Factor	Bearingless Hub with Dampers	Bearingless/ Damperless Hub
K_d	0.25, 1.0	0.3, 1.0
K_a	0.9998	0.9
K_d	13.21	17.5
K_w	-0.15	3.55
K_p	24.0	32.0
K_e	4.9	-5.44
K_m	12.7	107.76
K_b	-10.4	3.7
K_r	7.78	8.1
K_c	5.0	5.0
K_f	9.998	9.998
K_z	0	1.0
K_s	0	0
Merit Function	16.76, 67.02	49.46, 164.85

The minimum rotor hub moment merit factor for the damperless hub points out a problem with the definition of the merit factors. The rotor hub moment stiffness and minimum rotor hub tilt angle are sufficient to evaluate the hub concepts for their flapping characteristics. The damperless hub exceeded the rotor hub moment stiffness goal by 224 percent and has the ability to achieve a rotor hub tilt angle of 5.37 degrees at the endurance limit for graphite. Therefore, the resulting minimum rotor hub moment is a very large number, 215 percent of the goal. This unduly rewards the damperless hub for having a large rotor hub moment stiffness.

9. MANUFACTURING ASPECTS

The manufacturing plans for both hub configurations will be very similar. The approach for producing a limited number of prototype hubs will be to keep the tooling and work aids to a minimum. In a production environment, the approach will be to reduce the labor required through high-rate tooling and work cells for as-required prefabrication of small parts (no cold storage requirements for perishable subassemblies).

The yokes of both hub configurations will be made of belts of unidirectional material that are interleaved with tape in the center section. The number of belts was kept to a minimum (16 belts for each hub) to reduce the winding and layup time. The belts will be wound in four basic lengths to accommodate the precone and placed into a shaping tool for debulking under mechanical pressure. The belts for both hub configurations will have thickness and width transitions for the center section. Tape reinforcements are added at the loop ends for the blade attachment.

The material used for the buildup of the center section, flap flexure, and loop ends is a mixture of unidirectional and ±45 degree tape. Fabric will be used to stabilize the geometry of the pitch change element. The number of ply dropoffs will be kept to a minimum to reduce the number of discrete plies and to increase the number of ply stock assemblies. There will be over 200 plies that must be cut, laid up, and debulked for both yoke assemblies. In a production environment, the cutting of plies for several yoke assemblies could be done at the same time with a steel-ruled die cutter.

The plies of tape and fabric, belts, bushings, and precured fids (spacer or filler blocks of fabric/epoxy used for stabilizing bushings) will be placed into a bond fixture. There will be several intermediate debulking stages during the assembly of the yoke details to ensure dimensional control of the cured yoke. The bond fixture will be integrally heated and cooled under pneumatic top and side pressure to ensure tool closure. This is a more efficient means of applying temperature and pressure than the use of an autoclave.

The cured yokes will require very close tolerances for trimming and boring of bushings. The excess portions of the yokes that are trimmed will undergo shear tests to determine the integrity of the lamination. The other areas of the yokes will undergo X-ray and ultrasonic inspections to check for voids and foreign matter.

The cuffs for both hub configurations will be helically wound. For the bearingless hub with dampers, graphite roving will be wound at ±15 degrees (for chordwise stiffness) and ±45 degrees (for the torsional stiffness). For the damperless hub, fiberglass roving will be wound at ±45 degrees. The cuffs will be tooled to the inside surface with a steel mandrel that will serve for winding and curing. The mandrel will be made of several pieces that must be taken apart to remove the cuffs after curing. This is necessary due to the geometry of the cuffs for reduced drag. A 0.5-inch-thick 70-80 durometer silicone caul sheet will be installed over the outside surface before bagging. Blade attach lugs, fids, pitch horn attach bolt, and ±45 degree reinforcements will be installed on the cuff during helical winding. The cured cuffs will be trimmed and the surplus material used for shear tests. The cuffs will also be subjected to X-ray and ultrasonic inspections.

10. FRR VARIATIONS

Modifications to each of the basic ITR hub configurations for performance and stability investigations were examined. Mass and stiffness modifications for reduced loads and vibration could also be made. However, these modifications would have to be made in conjunction with the rotor blades for "nodalized rotor" investigations.

10.1 AERODYNAMIC VARIATIONS

Since both hub configurations use a cuff to introduce blade pitch, the aerodynamic variations of each hub would be similar. The existing yokes of the basic ITR hubs would be used for the FRR. The performance benefits associated with alternate cuff geometries could be investigated through flight research. The current cuffs were shaped for minimum download at high speed flight. This effect could be compared to cuff geometries of simpler elliptical cross sections. The current cuffs are tapered in height for reduced frontal area. This makes the cuffs more difficult to manufacture. Cuffs with constant cross sections could be tested on the FRR to determine if the drag reductions of the tapered cuffs would offset the manufacturing costs. Other cuff configurations could include tabs and fairings to provide cuff contours more representative of airfoils.

In addition to cuff variations, the effects of the blade bolt fairings could be investigated to determine if the additional parts and folding complications are offset by the reduction in drag. Another aerodynamic variation that could be incorporated for the FRR would be a fairing over the center section. However, the center section fairing and attachment hardware would impose additional parts and weight to the rotor system. Sealing the inboard end of the cuffs would provide favorable aerodynamics but would not be practical because of the relative motions between the cuffs and the yoke.

Figure 26 shows one possible aerodynamic FRR configuration incorporating the variation described above for the bearingless hub with dampers. Figure 27 shows the bearingless/damperless hub with aerodynamically comparable variations for the FRR. These figures show the minimum size cuffs for the two hub configurations. With these cuffs as a baseline, fairings could be bonded on the leading and trailing edges to represent other cuff configurations.

Another item that could be investigated is simulated cuff feathering through circulation control of the cuffs. The cuffs would have slots with an air pumping mechanism. The air would be pumped in a manner to reduce the hub drag and download at high speed flight.

ORIGINAL PAGE IS
OF POOR QUALITY

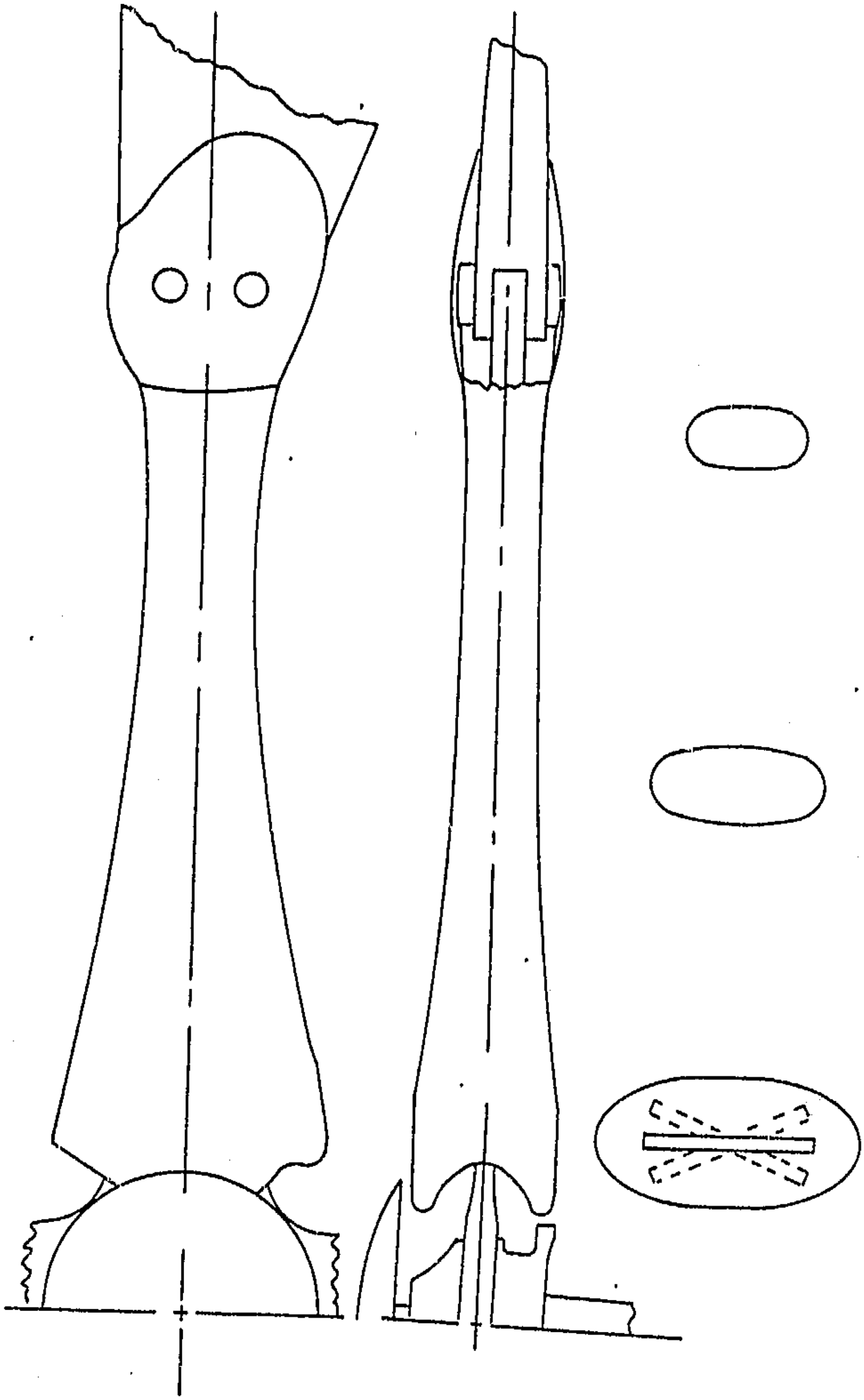

Figure 26. FRR Cuff Shape for Bearingless Hub With Dampers

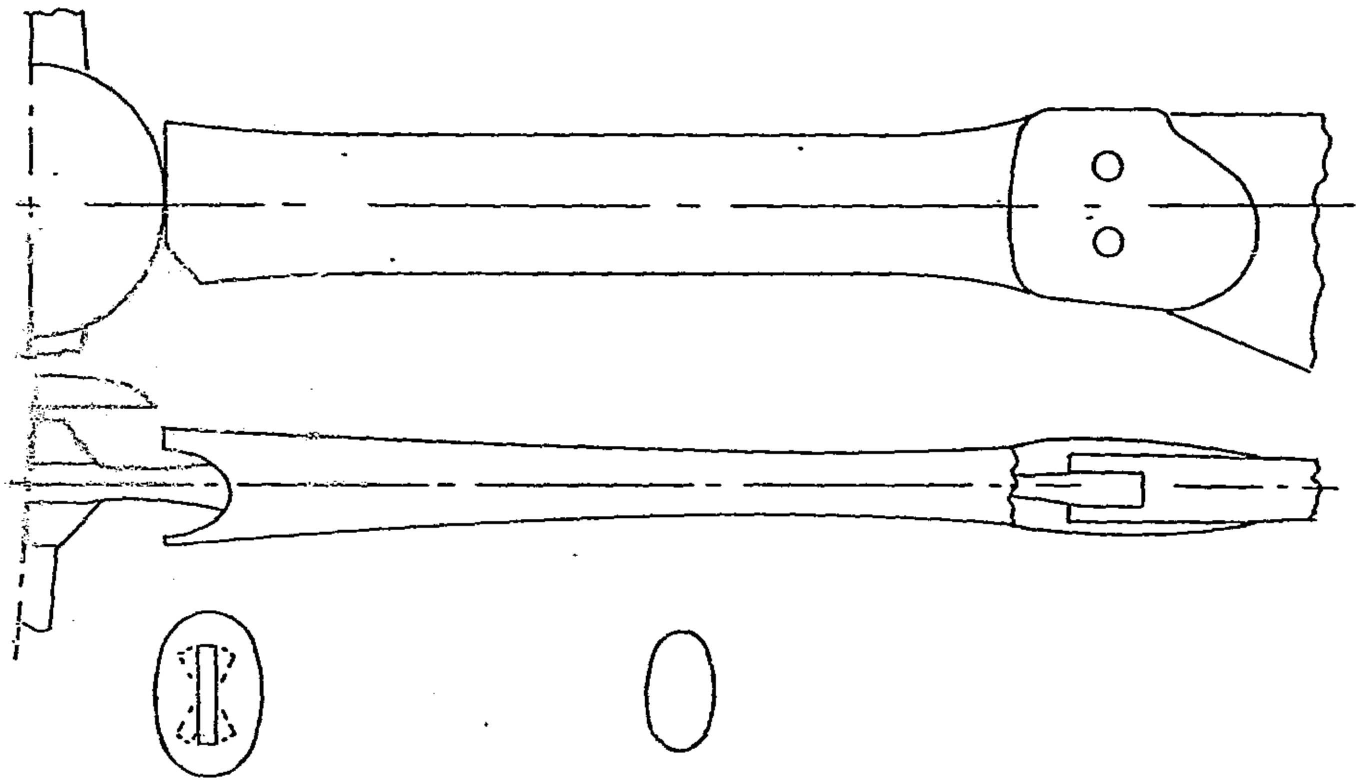

Figure 27. FRR Cuff Shape for Bearingless Hub Without Dampers

10.2 STABILITY

The FRR hub variations that could be made for stability investigations can be divided into two categories: modifications involving the existing yokes of the basic ITR hub configurations and new yokes incorporating tooling inserts and material changes.

10.2.1 FRR Stability Variations for Bearingless/Damperless Hub

For the damperless hub, damper strips could be bonded to the existing yoke to provide some additional structural damping. Also, the cuff could be replaced with a torque tube to determine the effects of the cuff on the couplings. This would require a fitting at the blade attachment/torque tube interface and a new shear restraint that would be positioned below the yoke.

New yokes based on the tooling of the damperless hub could be made to investigate different aeroelastic couplings. The twist of the yoke and stiffness distributions could be varied. Also, a hybrid yoke with elastomeric material within the structure could be evaluated. These modifications would require additional manufacturing work aids such as templates, debulking tools, winding tools, planning and quality control procedures, and main bond tool inserts.

10.2.2 FRR Stability Variations for Bearingless Hub with Dampers

For the bearingless hub with dampers, the damper properties and yoke stiffness distribution would be optimized during detail design. Therefore, adding damper strips or altering the yoke geometry would compromise the efficiency of the damper; thus, the effort focused on removing the dampers while supplying a mechanism for stability. Since the elastic spring rates of the dampers supply a significant amount of stiffness to this hub configuration, a means of replacing the lost stiffness is also necessary.

Figure 28 shows a possible damperless configuration. The cuff would be replaced with a torque tube that is connected to a linkage arrangement instead of a simple pivot for the shear restraint. The pitch link will go through a hole in the flexure of the yoke. As the rotor blade lags, the torque tube will move inboard. The linkage will force the torque tube down with the inboard motions. Since the pitch link/pitch horn attachment does not move, the rotor blade will increase pitch with the lagging motion. Consequently, the rotor blade pitch will decrease when the blades lead. This concept appears to be an effective way to introduce a significant amount of pitch-lag coupling through the linkage arrangement and is independent of the hub moment stiffness and the geometry of the pitch change portion of the yoke.

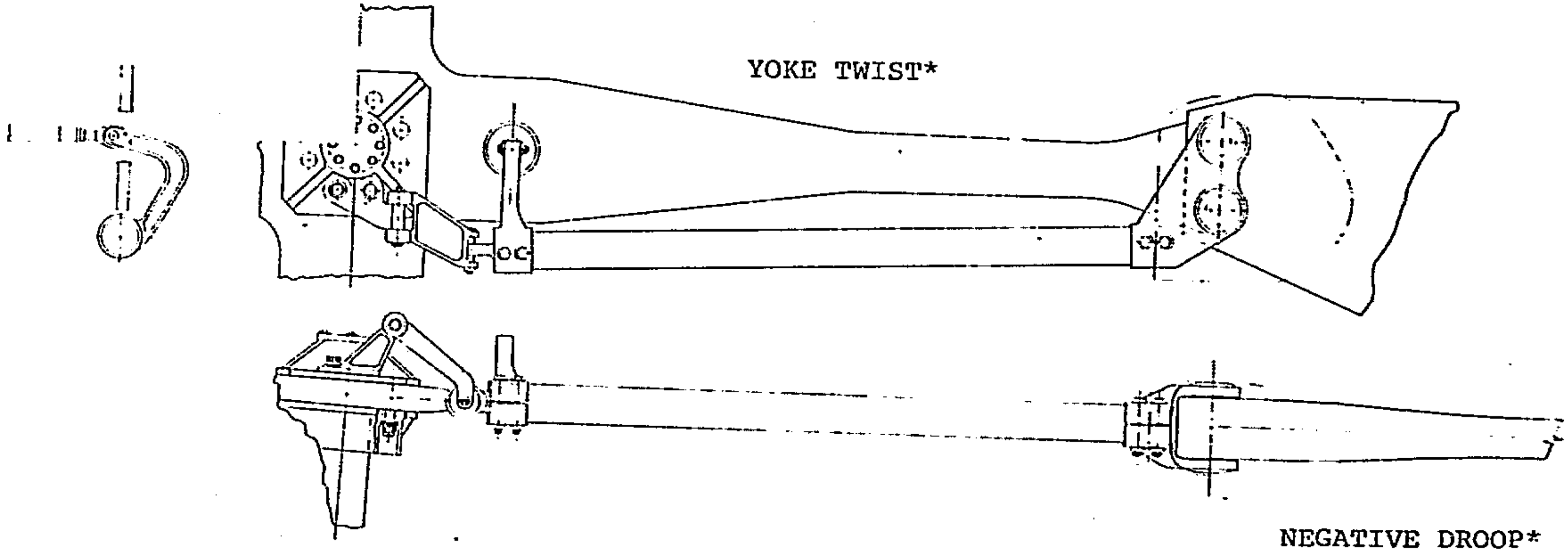

*COULD BE INCORPORATED IF NECESSARY

Figure 28. Damperless Hub With Pitch-Lag Coupling Mechanism

To achieve the desired inplane natural frequency with the existing yoke tool, the material must be changed to make up for the stiffness of the dampers. If graphite were used for the entire yoke, the inplane natural frequency would be too large (0.8 per rev) because of the long and relatively wide flap flexure. Also, the hub moment stiffness would be significantly increased. However, a mixture of graphite and fiberglass could provide an acceptable design. Since this yoke design uses sets of four belts of unidirectional material stacked vertically, the middle belts could be graphite and the surface belts could be fiberglass. This combination of material would increase the chordwise stiffness distribution of the original yoke by the average modulus of graphite and fiberglass. There would be a negligible increase in the beam stiffness distribution with the graphite in the middle of the flap flexure. The torsional stiffness would not be increased because the radius of gyration of the pitch change element is unchanged and the shear modulus of graphite is very close to fiberglass (see Table VI).

This new concept was developed very late in this program and is considered as an FRR variation of the bearingless hub with dampers. More refinement of this concept would be necessary to ensure its feasibility. The parts and weight of the linkages and pivot bearings need to be assessed and a means of reducing the hub drag needs to be investigated. If this new hub concept is treated as a candidate hub for the ITR, yoke twist for flap-lag coupling should be incorporated. The flap flexure must also have the ability to withstand the droop loads and limit the droop excursions. Negative droop could be incorporated at the blade attachment to augment the pitch-lag coupling and help limit the droop excursions.

11. RSRA COMPATIBILITY

The rotor speed of the RSRA must be changed for compatibility with the ITR. This can be accomplished by a new freewheel unit mesh with a reduction ratio of 2.04. This will provide a rotor speed of 252 rpm, which would accommodate both hub configurations.

Since the ITR will be a four-bladed rotor system, new rotating controls will be required. The swashplate and pitch links must be sized for the pitch horn geometries of the ITR hubs and must be able to withstand the flight loads that the rotor will experience. A new mast will also be required. The size of the mast will be influenced by the hub moment stiffness. This will imply a thicker mast for the damperless design. Also, the transmission upper case, bearings, and airframe attachments must be checked.

Other items that will require investigation are the airframe dynamics for stability, flight loads, and vibration. The anticipated rotor hub tilt angles must be determined for the ITR on the RSRA. The influence of the airframe drag, elevator incidence, and center-of-gravity must be addressed.

Finally, the handling qualities of the RSRA with the ITR will require investigation. The control system phasing must be matched with the pitch-flap couplings of the ITR hubs. The fixed system control travels must be assessed and the ability to reverse the controls for leading or trailing edge pitch horns will be required, depending on the final hub configuration.

12. CONCLUDING REMARKS

This concept definition predesign study for the ITR/FRR program provided the opportunity to generate candidate hub concepts. These concepts were evaluated to determine how well the project objectives will be met.

The eight potential concepts that were considered early in the program covered a wide spectrum. Hub concepts with and without pitch change bearings were considered. These concepts were qualitatively rated on their potential to meet the ITR/FRR objectives. The design that rated the highest was a bearingless hub with elastomeric dampers. This hub concept was selected for further development and evaluation. A bearingless/damperless hub concept was also selected because of its potential for reduced parts count, weight, and cost, even though it was judged to have greatest risk.

The bearingless hub with dampers was refined to maximize its flapping ability and damper efficiency. It evolved to a fiberglass yoke with a thin flap flexure and a graphite cuff. The advantages of this hub configuration are its stability, low hub moment stiffness, and fail-safe yoke. The disadvantages are the additional parts count due to the dampers and the need of a droop stop (formed by extensions of the lower clamp plate and cuffs).

The damperless hub concept evolved from a design with a fiberglass yoke and a graphite torque tube to a graphite yoke and fiberglass cuff. The advantages of this hub configuration are its low parts count and weight. The disadvantages are the risks of instability, relatively high hub moment stiffness, and the failure modes associated with the graphite in the yoke.

Both hub configurations have a significant amount of graphite that must be protected from lightning strikes on the rotor blades. This can be done by conductive coatings and grounding wires from the abrasion strip of the blades to the pitch link attachments.

The hub concept that was developed as an FRR variation of the bearingless hub with dampers has the potential to produce a significant amount of pitch-lag coupling independently of the hub moment stiffness. This concept would require more refinement before it could be considered as an ITR hub. However, it is a viable FRR candidate of the bearingless hub with dampers because it will not require a new yoke bond tool.

RSRA modifications would be required of the transmission and rotating controls for installation of the ITR. The ITR hub concepts should be compatible with the RSRA.

LIST OF SYMBOLS

A	area, in^2
C/C_c	damping ratio
CF	centrifugal force, lb
C_T	thrust coefficient
D	diameter, in
EIB	beam stiffness, $lb\text{-}in^2$
EIC	chord stiffness, $lb\text{-}in^2$
G'	elastic shear modulus lb/in^2
GI	generalized inertia, $in\text{-}lb\text{-}sec^2$
K'	elastic spring rate, lb/in
$\bar{K}$	radius of gyration, in
KG	shear rigidity, $lb\text{-}in^2$
R	rotor radius, in
t	thickness, in
t_c	rotor thrust coefficient
W	width, in
γ	loss tangent
ζ	damper displacement, in
ε	strain, in/in
μ	advance ratio
σ	solidity
τ	shear stress, lb/in^2
ω	natural freqeuncy, rad/sec

APPENDIX

For the convenience of the reader, the hub specifications, goals, and merit function definitions which appeared in RFQ DAAK51-81-Q-0054 as Appendixes B and C are included here.

ROTOR HUB DESIGN SPECIFICATIONS

The following rotor hub design specifications establish minimum requirements to be used to guide the design of the rotor hub. The hub design specifications have been derived from the ITR System Design Specification, specialized as appropriate for the development of hub components within the scope of the Concept Definition work.

Design Gross Weight - The ITR design gross weight shall be not less than 16,000 pounds and not more than 23,000 pounds. The specification requires that the ITR rotor be designed to have the thrust capability to permit the vehicle to hover OGE at 4000 feet pressure altitude and 95°F with a total vehicle weight equal to the design gross weight plus a 10 percent fuselage download penalty.

Design Envelope - For the purposes of the rotor hub design, the structural design envelope is +3.5g and -0.5g. Slope landing conditions up to and including 12 degrees shall be accommodated.

Rotor System Instability - The rotor and test aircraft shall be free of critical aeroelastic and mechanical instabilities at all operating conditions and throughout a typical range of gross weights. For the purpose of air/ground resonance instability, the rotor hub design requirements shall be consistent with fuselage and blade mass and inertia characteristics typical of the design gross weight.

Rotor Hub Configuration - It is desired that the rotor be a four-bladed system. The hub design shall not preclude the incorporation of normal operational requirements for simple and quick manual blade folding and blade removal or replacement which does not require retracking or rebalancing. The hub design concept shall not be so restrictive or unconventional that it would be incompatible with the incorporation of provisions for surviving limited wire strikes (0.25-inch copper nonshielded wires) and combat damage (minimum probability of catastrophic failure following hit by 23-mm HEI projectiles).

ROTOR HUB TECHNICAL GOALS

a. Rotor hub flat plate drag area.	2.8 ft^2
b. Rotor hub weight as a percentage of design gross weight.	2.5 pct
c. Rotor hub system parts count, exclusive of standard fasteners.	50
d. Rotor hub moment stiffness. Defined by the moment in ft-lb, acting at center of the hub, per unit angular rotation in radians of the rotor disc about an axis perpendicular to the rotor shaft axis. The rotor disc is defined by the circle inscribed by hypothetical rigid blade tips.	150,000 ft-lb/rad
e. Minimum rotor hub moment. The minimum rotor hub moment in ft-lb, acting at the center of the rotor hub, below which fatigue damage will not be incurred by the hub.	10,000 ft-lb
f. Minimum rotor hub tilt angle. The minimum rotor disc angle defined in paragraph d above, below which fatigue damage will not be incurred by the rotor hub.	5 deg
g. Auxiliary lead-lag damping. The goal of the ITR is to develop a rotor system that does not require auxiliary hydraulic or elastomeric damper components incorporated in the hub. It is desirable to have the potential of incorporating some form of additional damping, if at some later stage in the development process it appears prudent to do so in order to solve an emerging stability problem.	---
h. Torsional stiffness. The technical goal is to develop a rotor hub system that does not require substantially more blade pitch control actuator force than required by current rotor systems.	---
i. Rotor hub system fatigue life.	10,000 hr
j. Reliability. Mean-time-between-removal (MTBR) for the hub.	3,000 hr

k. Manufacturing cost. The ITR rotor system will be designed to provide the lowest possible procurement cost for future production rotors based on ITR technology, without unduly compromising other cost factors that impact optimum life cycle costs.

MERIT FACTORS/MERIT FUNCTION

a. Vulnerability to 23-mm HEI projectile	K_v - probability of surviving hit
b. Risk of aeromechanical instability	K_a - probability that rotor system will be free from air/ground resonance instability
c. Hub drag area	K_d - % reduction from technical goal
d. Hub weight	K_w - % reduction from technical goal
e. Part counts	K_p - % reduction from technical goal
f. Rotor hub moment stiffness	K_e - equal to 5 if rotor hub moment stiffness is within ±20% of the technical goal. K_e is reduced from 5 by one-tenth of the percentage that the parameter exceeds a ±20% margin from the goal
g. Minimum rotor hub moment	K_m - one half of the percentage by which the parameter exceeds the technical goal
h. Minimum rotor hub tilt angle	K_b - one half of the percentage by which the parameter exceeds the technical goal
i. Reliability	K_r - ten times the probability of meeting or exceeding technical goal for MTBR
j. anufacturing cost	K_c - qualitative estimate from 1 to 10, varying inversely with expected cost
k. Fatigue life	K_f - ten times the probability of meeting or exceeding the technical goal
l. Auxiliary lead-lag damping	K_z - 0 to 2, qualitative estimate of practicality of incorporating auxiliary damping

m. Torsional stiffness

K_s - if pitch control system forces exceed of 1.5 times typical pitch bearing hub $K_s = -2$; if forces less than this level, $K_s = 0$

Merit Function

$$= K_v \times K_a \times (K_d + K_w + K_p + K_e + K_m + K_b + K_r + K_c + K_f + K_z + K_s)$$